Transp Porous Med (2013) 96:369–396
DOI 10.1007/s11242-012-0093-y

Effective Stress in Unsaturated Soils: A Thermodynamic Approach Based on the Interfacial Energy and Hydromechanical Coupling

Ehsan Nikooee · Ghassem Habibagahi · S. Majid Hassanizadeh · Arsalan Ghahramani

Received: 4 April 2012 / Accepted: 19 October 2012 / Published online: 8 November 2012

Abstract In recent years, the effective stress approach has received much attention in the constitutive modeling of unsaturated soils. In this approach, the effective stress parameter is very important. This parameter needs a correct definition and has to be determined properly. In this paper, a thermodynamic approach is used to develop a physically-based formula for the effective stress tensor in unsaturated soils. This approach accounts for the hydro-mechanical coupling, which is quite important when dealing with hydraulic hysteresis in unsaturated soils. The resulting formula takes into account the role of interfacial energy and the contribution of air–water specific interfacial area to the effective stress tensor. Moreover, a bi-quadratic surface is proposed to represent the contribution of the so-called suction stress in the effective stress tensor. It is shown that the proposed relationship for suction stress is in agreement with available experimental data in the full hydraulic cycle (drying, scanning, and wetting).

Keywords Effective stress parameter · Entropy inequality · Interfacial energy · Hydro-mechanical coupling · Air water specific interfacial area · Suction stress characteristic surface (SSCS)

1 Introduction

1.1 Effective Stress Approach

The concept of effective stress was introduced by Terzaghi (1936) as one of the fundamental concepts of saturated soil mechanics. Since then, many attempts have been made to extend

E. Nikooee (✉) · G. Habibagahi · A. Ghahramani
Department of Civil and Environmental Engineering, Shiraz University,
P.O. Box 7134851156, Shiraz, Iran
e-mail: ehsan_nikooee@yahoo.com; nikooee@shirazu.ac.ir

S. M. Hassanizadeh
Earth Sciences Department, Utrecht University,
P.O. Box 80021, 3508 TA Utrecht, The Netherlands

this concept to unsaturated soils (see e.g., Bishop 1959; Bishop and Blight 1963; Kohgo et al. 1993; Khalili and Khabbaz 1998; Khalili et al. 2004; Nuth and Laloui 2008a; Laloui and Nuth 2008; Khalili and Zargarbashi 2010; among many others). The effective stress is a combination of the total stress and the fluid phase pressures inside a porous material; it is the stress that governs the mechanical behavior of the porous material (in our case, soil). According to Khalili et al. (2004), the concept of effective stress "*converts a multi-phase multi-stress state porous medium to a mechanically equivalent, single-phase, single-stress state continuum allowing the application of the principles of continuum solid mechanics.*" That is why there has been a great appeal to extend this concept to unsaturated soils where more than one fluid phase exists.

In the pioneering work of Bishop (1959), the following formulation was introduced for the effective stress in unsaturated soil mechanics:

$$\sigma'_{ij} = (\sigma_{ij} - P^a \delta_{ij}) + \chi \; P_c \delta_{ij} \tag{1}$$

where σ_{ij} is the total stress tensor, P^a is the air pore pressure, χ is the so-called effective stress parameter, and P_c is the matric suction (capillary pressure), and δ_{ij} denotes the unit tensor. One of Bishop's recommendations for the effective stress parameter was to set it equal to the degree of saturation of water (or the wetting phase in general). Since then, this simple suggestion has been used in many studies such as the works of Schrefler (1984), Jommi and di Prisco (1994), and more recently Laloui and Nuth (2008).

After Bishop's proposal for the effective stress formula, during the past five decades, there has been much debate on the application of effective stress concept as well as the appropriate choice of effective stress parameter and its formulation in unsaturated soils. This debate has led to different approaches, advantages and disadvantages of which have been presented in a comprehensive review elsewhere (Nuth and Laloui 2008a). Recently, it has been shown that the effective stress approach can model the unsaturated soil behavior provided that it is used within a proper constitutive framework (Loret and Khalili 2000; Khalili et al. 2004; Nuth and Laloui 2008a; Alonso et al. 2010). Nonetheless, there are still open questions to which the current study is devoted. Despite the recent progress on the application of effective stress approach for modeling the behavior of unsaturated soils, the most proper choice of effective stress parameter is not clearly known. Results of recent studies show that the effective stress parameter cannot be simply taken as the degree of saturation (see e.g., Khalili and Zargarbashi 2010; Alonso et al. 2010; Pereira et al. 2010). The focus of these studies has been on finding alternative formulas for the effective stress parameter.

Recently, published studies have shown the importance of hydro-mechanical coupling, the effect of hydraulic hysteresis on the effective stress, as well as the role of bonding phenomenon. Hence, the essential question is whether other terms should be present in the effective stress formulation. To the best of authors' knowledge, there is no comprehensive theoretical work in the literature to address this question, specifically from a thermodynamic standpoint. In particular, previous thermodynamic approaches have not fully investigated the variation of the effective stress for a complete hydraulic cycle. In a full hydraulic cycle, air–water interfaces are expected to play a major role and additional terms are required to take into account their influence.

In a porous medium, the interplay of all phases and interfaces governs the overall mechanical behavior. However, in the current formulations, while the fluid phase pressures and their corresponding saturation appear in the effective stress formulation, there is no term related to interfaces. But, one would intuitively expect fluid–fluid and solid–fluid interfaces to contribute to the effective stress formulation as well. The trends and phenomena observed in

recent experiments confirm this expectation. These phenomena are briefly reviewed in the following section.

In what follows, we focus on the role of fluid–fluid interfaces in effective stress formulation. But as discussed in "Appendix B", solid–fluid interfaces can also contribute to effective stress formulations, particularly, when grains are considered to be deformable.

1.2 Review of Recent Experimental Evidences: Role of Various Physical Phenomena

1.2.1 Role of Hydraulic History

The importance of hydraulic history in hydro-mechanical behavior of unsaturated soils has been understood only recently (Khalili and Zargarbashi 2010; Uchaipichat 2010a,b). These studies show that the value of the effective stress parameter at a given matric suction is different when different hydraulic paths (drainage or imbibition) are followed to reach that matric suction.

Experimental studies of Khalili and Zargarbashi (2010) confirmed that the effective stress parameter is not equal to the degree of saturation unless there is an additional term in the effective stress formulation. They showed that the effective stress parameter can decrease following a wetting scanning curve, where the degree of saturation remains nearly constant. There is no theoretical investigation on this important phenomenon and its underlying mechanisms. Khalili and Zargarbashi (2010) conjectured that this phenomenon can be attributed to the effect of air–water interface but they did not indicate how air–water interface can be included in the effective stress formulation.

1.2.2 Role of Capillary Forces (Bonding Phenomenon)

Air–water interfaces are also expected to play a role in the description of bonding effects and capillary forces. Capillary forces are exerted by the contractile skin on the soil grains. The outcome is an increase in the inter-granular forces which resist grain sliding under external forces. This physical effect of capillary forces has been called bonding effect in the literature (Nuth and Laloui 2008a); here, we refer to it as the bonding phenomenon.

Previous micro-mechanical investigations of a wet granular medium have indicated that capillary forces need to be incorporated in the formulations of the mechanics of unsaturated soils (Chateau and Dormieux 2002; Lu and Likos 2006). Thus, one would expect the capillary forces to make significant contributions to the effective stress tensor in partially saturated soils. However, since their contribution is not fully known and it is hard to measure, they are usually overlooked in the effective stress formulations.

It is noteworthy that the importance of bonding phenomenon was already understood at the early stages of soil mechanics. Terzaghi (1943) devoted a chapter to capillary forces in his famous textbook (Theoretical Soil Mechanics, Chapter 14). Illustrations on the contribution of capillary forces date back to 1960s, for instance, in works of Blight (1961) and Matyas and Radhakrishna (1968). More fascinating, it was conjectured that the bonding phenomenon is related to the amount of air–water interface (Blight 1961; Matyas and Radhakrishna 1968). However, they did not elaborate on how the bonding effects should be measured or how such dependency could be specified. Their suggestion has never been examined by the soil mechanics community as air–water interface itself was an unfamiliar state variable and could add to the complexity of the problem description. Therefore, both early works and recent micro-mechanical studies point out the importance of capillary forces in the mechanical behavior

of soil and their potential relation to the amount of air–water interface. Such interconnection is not well known and needs to be investigated.

1.2.3 Hydro-mechanical Coupling

A fully coupled unsaturated model not only needs a complete understanding of stress tensors and forces inside medium but also should account for their influence on the free energy of different phases and interfaces. The two aspects mutually affect and complement one another.

The effect of state of stress on water saturation is now well established. Nuth and Laloui (2008b), Masın (2010), and Uchaipichat (2010c) have shown that the soil water retention curve clearly depends on the state of stress. In other words, these studies reveal that a change in the porosity of soil as a result of a change in the stress level can bring about changes in the water retention behavior of the soil. This dependency, which is usually known as the hydro-mechanical coupling, has exclusively been examined for the variation of degree of saturation with suction (soil water retention curve) at different levels of net stress. An important question is whether there is a hydro-mechanical coupling between the amount of interfacial energy and the state of stress and how this dependency can be included in a hydro-mechanical modeling. In other words, one may expect the interfacial energy, which has a close relationship with the evolution of interfaces in different hydraulic paths (drying, wetting and scanning), to be a function of soil structure and can consequently vary as the soil deforms. Such interconnection is important and proper inclusion of such dependency is expected to result in an enhanced form of the effective stress tensor. These important aspects and research questions are investigated in the course of this paper.

In order to address the aforementioned questions, a theoretical framework is required. The framework based on which the current study is found to be a rational thermodynamic approach. Before entering the theoretical details, the essential elements and key requirements of such framework are briefly introduced in the next section.

1.3 Requirements for a Proper Thermodynamic Approach for Unsaturated Soils

Given the fact that solid–fluid interactions as well as contractile skin forces are interfacial phenomena, one would expect a state variable representing interfaces to be included in a thermodynamic theory of hydro-mechanical coupling. Thus, we submit that a proper theory of unsaturated soil mechanics should account for the following three issues:

1. Inclusion of thermodynamics properties of the interfaces. For this purpose, appropriate and well-posed balance laws for the interfaces should be defined at micro-scale followed by a proper upscaling to the macro-scale level. This is, indeed, an important prerequisite for a proper definition of stress tensors.
2. Incorporation of coupled phenomena which are observed at macro-scale in the definition of dependencies and constitutive equations.
3. Verification of the results of the theory and their interpretation against the trends observed in available experimental data.

There exist thermodynamic approaches in the literature which have considered the interfacial effects. However, they did not address the above-mentioned issues in a comprehensive manner. Following is a brief description of some of these works.

A major contribution to poromechanical behavior of unsaturated media was made by late prof. Coussy in his last book (Coussy 2010). In fact, he is one of the first researchers

who noted the importance of interfaces in poromechanical behavior of unsaturated media. In the pioneering work of Coussy and Dangla (2002), they considered relevant terms in the free energy of skeleton to take into account the interfacial effects in the effective stress tensor. However, they did not introduce balance laws for interfaces. Their major assumptions, and main difference between their approach and the current study are discussed later in Sects. 2.5 and 3.2.

Hassanizadeh and Gray (1990) developed a thermodynamic approach for multiphase flow in porous media. They obtained a Bishop's type equation with the effective stress parameter equal to the degree of saturation. This type of equation does not fully agree with recent experimental observations. A careful exploration of their work reveals that their approach lacks a proper hydro-mechanical coupling. This issue is explained in detail in the subsequent sections.

Through a thermodynamic approach, Gray and Schrefler (2001) studied the solid–fluid interfacial effects. They also obtained a Bishop's type formulation for the effective stress with the wetted fraction of the grains as the effective stress parameter together with some additional terms related to the grain curvature. In their formulation, there was no term to account for the bonding effects.

Almost all other thermodynamic approaches employed to study the effective stress and mechanical energy of unsaturated soils did not take into account the interfacial energy, or at least neglected it at some point in their formulations. Some of those studies include Houlsby (1997), Hutter et al. (1999), Borja (2006), Zhao et al. (2010), and Lu et al. (2010).

The framework proposed in this study considers the aforementioned requirements. It aims at the inclusion of hydro-mechanical coupling in the effective stress formula through a rational thermodynamic approach.

The proposed framework results in a new equation for the effective stress tensor. It demonstrates that a Bishop's type formulation for the effective stress needs additional terms which make it capable of describing the phenomena introduced before. We describe how the additional term(s) are well connected to the above-mentioned trends and are physically plausible. The terms introduced in this study account for the effects of interfacial energy and bonding phenomenon.

As a further outcome, the new concept of *suction stress characteristic surface* (SSCS) is introduced and a general formulation for the effective stress parameter is offered. In addition, it is discussed how the proposed formulation reduces to some of the previously presented equations with certain assumptions.

The structure of the paper is as follows. First, the utilized theoretical framework is described. Next, the proposed equations are used to explain results of experiments over a full hydraulic cycle and for different soil samples. Afterwards, a discussion on the results and merits of the proposed equations are presented. Finally, concluding remarks and a number of suggestions are set forth for future studies.

2 Theory

2.1 Outline of the Method

In the derivation of the formulation for the effective stress tensor, the upscaled balance laws for phases and interfaces inside unsaturated soil will be employed. Application of balance of mass, momentum, entropy, and energy for phases and interfaces along with the second law of thermodynamics (also known as the entropy inequality), combined with constitutive

assumptions for hydro-mechanical coupling, will lead to a new formula for the effective stress tensor. First, these equations and laws are briefly described in the following sections.

2.2 Balance Laws for Phases and Interfaces

In this study, two fluid phases (wetting and nonwetting fluid phases) are considered, hereafter denoted by w and n, respectively. There is also a third phase which is the soil skeleton, denoted by s. These phases are in contact with each other through three interfaces which are: solid–wetting fluid interface, denoted by ws; solid–nonwetting fluid interface, specified by ns; and fluid–fluid interface, denoting by wn. To specify a phase, Greek letter α or β is used. There exists also a common line, denoted by wns, where all phases and interfaces come together. Interfaces exchange mass, momentum, energy, and entropy with each other through the common line only.

The notation of material derivative appears in balance equations. Material derivative of a function ψ is defined as follows:

$$\frac{\mathrm{D}^{\alpha}\,\psi}{\mathrm{D}t} = \frac{\partial\,\psi(\mathbf{x},t)}{\partial t} + \mathbf{v}^{\alpha}\cdot\nabla\,\psi(\mathbf{x},t). \tag{2}$$

Following Hassanizadeh and Gray (1990), the following macroscale equations of balance have been used in this study:

2.2.1 Conservation of Mass

For solid phase:

$$\frac{\mathrm{D}^{s}(1-\varepsilon)\rho^{s}}{\mathrm{D}t} + (1-\varepsilon)\rho^{s}(\nabla\cdot\mathbf{v}^{s}) = \hat{e}^{s}_{ns} + \hat{e}^{s}_{ws} \tag{3}$$

For fluid phases:

$$\frac{\mathrm{D}^{\alpha}(\varepsilon s^{\alpha}\rho^{\alpha})}{\mathrm{D}t} + \varepsilon s^{\alpha}\rho^{\alpha}(\nabla\cdot\mathbf{v}^{\alpha}) = \sum_{\beta\neq\alpha}\hat{e}^{\alpha}_{\alpha\beta} \quad \alpha = n, w \tag{4}$$

For an interface:

$$\frac{\mathrm{D}^{\alpha\beta}(a^{\alpha\beta}\Gamma^{\alpha\beta})}{\mathrm{D}t} + a^{\alpha\beta}\Gamma^{\alpha\beta}(\nabla\cdot\mathbf{w}^{\alpha\beta}) = -\hat{e}^{\alpha}_{\alpha\beta} - \hat{e}^{\beta}_{\alpha\beta} + \hat{e}^{\alpha\beta}_{\alpha\beta\gamma}\ \alpha\beta = wn,\ ws,\ ns\ \ \alpha\beta\gamma = wns \tag{5}$$

where, ε denotes porosity, ρ^{α} specifies the density of α phase, $\mathbf{v}$ and $\mathbf{w}$ denote the average velocities of phases and interfaces, respectively, and Γ stands for the areal mass density of an interface. In general, a carat is used to designate exchange quantities. Thus, $\hat{e}^{\alpha}_{\alpha\beta}$ denotes the rate of mass exchange between an interface $\alpha\beta$ and a phase α and $\hat{e}^{\alpha\beta}_{\alpha\beta\gamma}$ shows the mass exchange between a common curve and an interface. Furthermore, s^{α} is the saturation of the α phase, and $a^{\alpha\beta}$ is the specific interfacial area of $\alpha\beta$-interface (amount of interface area per volume of REV). It is noteworthy that the saturation introduced in the equations is Eulerian saturation which is defined as the ratio of wetting phase volume to void volume in the deformed configuration (Coussy 2007).

A short description of the interfacial mass density, $\Gamma^{\alpha\beta}$, is presented hereafter. An interface is a transition zone between two bulk phases. There is a finite number of molecules associated with this transition zone. The mass of these molecules within an REV is equal

to $a^{\alpha\beta}\ \Gamma^{\alpha\beta}V_{\mathrm{REV}}$, where V_{REV} denotes the volume of REV. A rigorous exposition of this concept is given in Murdoch and Hassanizadeh (2002).

2.2.2 Conservation of Momentum

For a bulk phase (solid, fluids):

$$\varepsilon^{\alpha}\rho^{\alpha}\frac{\mathrm{D}^{\alpha}\mathbf{v}^{\alpha}}{\mathrm{D}t} - \nabla\cdot(\varepsilon^{\alpha}\mathbf{t}^{\alpha}) - \varepsilon^{\alpha}\rho^{\alpha}\mathbf{g}^{\alpha} = \sum_{\beta\neq\alpha}\hat{\mathbf{T}}^{\alpha}_{\alpha\beta} \quad \alpha = n, w, s \tag{6}$$

For an interface:

$$\begin{aligned} &a^{\alpha\beta}\Gamma^{\alpha\beta}\frac{\mathrm{D}^{\alpha\beta}\mathbf{w}^{\alpha\beta}}{\mathrm{D}t} - \nabla\cdot(a^{\alpha\beta}\mathbf{S}^{\alpha\beta}) - a^{\alpha\beta}\Gamma^{\alpha\beta}\mathbf{g}^{\alpha\beta} \\ &= -(\hat{\mathbf{T}}^{\alpha}_{\alpha\beta} + \hat{e}^{\alpha}_{\alpha\beta}\mathbf{v}^{\alpha,s}) - (\hat{\mathbf{T}}^{\beta}_{\alpha\beta} + \hat{e}^{\beta}_{\alpha\beta}\mathbf{v}^{\beta,s}) + (\hat{e}^{\alpha}_{\alpha\beta} + \hat{e}^{\beta}_{\alpha\beta})\mathbf{w}^{\alpha\beta,s} + \hat{\mathbf{S}}^{\alpha\beta}_{\alpha\beta\gamma} \quad \alpha\beta \\ &= wn, ws,\ ns \quad \alpha\beta\gamma = wns \end{aligned} \tag{7}$$

where ε^{α} is volume fraction of phase α, $\mathbf{g}^{\alpha}$ is the external supply of momentum, $\hat{\mathbf{T}}^{\alpha}_{\alpha\beta}$ denotes the momentum supply from interface $\alpha\beta$ to phase α, $\hat{\mathbf{S}}^{\alpha\beta}_{\alpha\beta\gamma}$ specifies momentum exchange between a common line and an interface, $\mathbf{t}^{\alpha}$ is the macroscopic stress tensor of phase α and $\mathbf{S}^{\alpha\beta}$ is the macroscopic stress tensor of interface $\alpha\beta$. For simple interfaces, $\mathbf{S}^{\alpha\beta}$ merely consists of the interfacial tension. But, in general one may have surface viscosity for fluid–fluid interfaces and surface strains for solid–fluid interfaces (for detailed explosion of interfacial mechanics, see Scriven 1960; Gurtin and Murdoch 1974; Hassanizadeh and Gray 1993; Cammarata and Sieradzki 1994; Spaepen 2000).

It must be noted that the momentum balance equations are not used explicitly in our derivation. But, they are used in reducing the general form of the energy balance equations to the ones introduced below (see Hassanizadeh and Gray 1979 for details).

2.2.3 Conservation of Energy

For a bulk phase:

$$\varepsilon^{\alpha}\rho^{\alpha}\frac{\mathrm{D}^{\alpha}E^{\alpha}}{\mathrm{D}t} - \varepsilon^{\alpha}\mathbf{t}^{\alpha}:\nabla\mathbf{v}^{\alpha} - \nabla.(\varepsilon^{\alpha}\mathbf{q}^{\alpha}) - \varepsilon^{\alpha}\rho^{\alpha}h^{\alpha} = \sum_{\beta\neq\alpha}\hat{Q}^{\alpha}_{\alpha\beta} \quad \alpha = n,\ w,\ s \tag{8}$$

For an interface:

$$\begin{aligned} &a^{\alpha\beta}\Gamma^{\alpha\beta}\frac{\mathrm{D}^{\alpha\beta}E^{\alpha\beta}}{\mathrm{D}t} - a^{\alpha\beta}\mathbf{S}^{\alpha\beta}:\nabla\mathbf{w}^{\alpha\beta} - \nabla.(a^{\alpha\beta}\mathbf{q}^{\alpha\beta}) - a^{\alpha\beta}\Gamma^{\alpha\beta}h^{\alpha\beta} \\ &= -[\hat{Q}^{\alpha}_{\alpha\beta} + \hat{\mathbf{T}}^{\alpha}_{\alpha\beta}\cdot\mathbf{v}^{\alpha,\alpha\beta} + \hat{e}^{\alpha}_{\alpha\beta}(E^{\alpha,\alpha\beta} + 1/2(\mathbf{v}^{\alpha,\alpha\beta})^2)] \\ &\quad -[\hat{Q}^{\beta}_{\alpha\beta} + \hat{\mathbf{T}}^{\beta}_{\alpha\beta}\cdot\mathbf{v}^{\beta,\alpha\beta} + \hat{e}^{\beta}_{\alpha\beta}(E^{\beta,\alpha\beta} + 1/2(\mathbf{v}^{\beta,\alpha\beta})^2)] + \hat{Q}^{\alpha\beta}_{\alpha\beta\gamma} \\ &\alpha\beta = wn, ws,\ ns \quad \alpha\beta\gamma = wns \end{aligned} \tag{9}$$

where E^{α} and $E^{\alpha\beta}$ denote internal energy density of a phase and an interface, respectively, $\hat{Q}^{\alpha}_{\alpha\beta}$ is heat supply from interface $\alpha\beta$ to phase α and $\hat{Q}^{\alpha\beta}_{\alpha\beta\gamma}$ denotes heat supply to interface $\alpha\beta$ from common line $\alpha\beta\gamma$. Moreover, $\mathbf{q}$ denotes the heat vector and h is the external supply of energy.

2.2.4 Balance of Entropy

For a bulk phase (solid and fluids):

$$\varepsilon^{\alpha}\rho^{\alpha}\frac{\mathrm{D}^{\alpha}\eta^{\alpha}}{\mathrm{D}t}-\nabla.(\varepsilon^{\alpha}\boldsymbol{\varphi}^{\alpha})-\varepsilon^{\alpha}\rho^{\alpha}b^{\alpha}=\sum_{\beta\neq\alpha}\hat{\Phi}^{\alpha}_{\alpha\beta}\ +\Lambda^{\alpha}\quad\alpha=n,w,s \tag{10}$$

For an interface:

$$\begin{aligned}a^{\alpha\beta}\Gamma^{\alpha\beta}\frac{\mathrm{D}^{\alpha\beta}\eta^{\alpha\beta}}{\mathrm{D}t}-\nabla.(a^{\alpha\beta}\boldsymbol{\varphi}^{\alpha\beta})-a^{\alpha\beta}\Gamma^{\alpha\beta}b^{\alpha\beta}=-(\hat{\Phi}^{\alpha}_{\alpha\beta}+\hat{e}^{\alpha}_{\alpha\beta}\eta^{\alpha,\alpha\beta})\\ -(\hat{\Phi}^{\beta}_{\alpha\beta}+\hat{e}^{\beta}_{\alpha\beta}\eta^{\beta,\alpha\beta})+\hat{\Phi}^{\alpha\beta}_{\alpha\beta\gamma}+\Lambda^{\alpha\beta}\quad\alpha\beta=wn,ws,\ ns\quad\alpha\beta\gamma=wns\end{aligned} \tag{11}$$

where η is the internal entropy density (entropy per unit mass), Λ denotes the rate of net production of the entropy, $\boldsymbol{\varphi}$ denotes entropy flux vector, $\boldsymbol{\Phi}$ is entropy exchange term, and b specifies the external supply of entropy. No thermodynamic property for common lines has been assumed.

The assumption of no thermodynamic property for common lines brings about the following restrictions on the exchange terms:

$$\begin{aligned}&\sum_{\alpha\beta}\hat{e}^{\alpha\beta}_{wns}\ =0\\ &\sum_{\alpha\beta}(\hat{\mathbf{S}}^{\alpha\beta}_{wns}+\hat{e}^{\alpha\beta}_{wns}\mathbf{w}^{\alpha\beta})\ =0\\ &\sum_{\alpha\beta}[\hat{Q}^{\alpha\beta}_{wns}+\hat{\mathbf{S}}^{\alpha\beta}_{wns}\cdot\mathbf{w}^{\alpha\beta}+\hat{e}^{\alpha\beta}_{wns}[E^{\alpha\beta}+1/2(\mathbf{w}^{\alpha\beta})^2]]=0\\ &\sum_{\alpha\beta}(\hat{e}^{\alpha\beta}_{wns}\eta^{\alpha\beta}+\hat{\Phi}^{\alpha\beta}_{wns})=0.\end{aligned} \tag{12a–d}$$

2.3 Second Law of Thermodynamics

This law states that the rate of net production of entropy of the system should be non-negative under all conditions and all processes. The following form of entropy inequality holds for multiphase systems (Gray and Hassanizadeh 1989):

$$\Lambda=\sum_{\alpha}\Lambda^{\alpha}+\sum_{\alpha\beta}\Lambda^{\alpha\beta}\geq 0 \tag{13}$$

where Λ^{α} and $\Lambda^{\alpha\beta}$ are given by Eqs. 10 and 11, respectively. Assuming that the sole source of entropy fluxes are heat input and taking entropy external sources to be proportional to energy external sources (Eringen 1980; Bowen 1984; Hassanizadeh and Gray 1990) one may propose the following equations:

$$\begin{aligned}\boldsymbol{\varphi}^{\alpha}&=\tfrac{\mathbf{q}^{\alpha}}{\theta^{\alpha}}\quad b^{\alpha}=\tfrac{h^{\alpha}}{\theta^{\alpha}}\\ \boldsymbol{\varphi}^{\alpha\beta}&=\tfrac{\mathbf{q}^{\alpha\beta}}{\theta^{\alpha\beta}}\ b^{\alpha\beta}=\tfrac{h^{\alpha\beta}}{\theta^{\alpha\beta}}\end{aligned} \tag{14}$$

where θ stands for temperature. Next, the Helmholtz free energy functions of phases and interfaces are introduced in the following forms:

$$\begin{aligned}A^{\alpha}&=E^{\alpha}-\theta^{\alpha}\eta^{\alpha}\\ A^{\alpha\beta}&=E^{\alpha\beta}-\theta^{\alpha\beta}\eta^{\alpha\beta}.\end{aligned} \tag{15}$$

2.4 Hydro-mechanical Coupling and its Influence on Constitutive Assumptions for Free Energies

Constitutive assumptions are required to close the above-mentioned set of equations. Hassanizadeh and Gray (1990) demonstrated how the proper selection of constitutive assumptions can be a significant step. They obtained an extended form of Darcy's law for multiphase systems following a systematic and physically based selection of constitutive equations. However, as mentioned earlier, in their results, the effective stress parameter is equal to the saturation, which does not agree with experimental results. This shortcoming is a result of the constitutive assumptions on the dependencies of free energies which may still be improved. Here, we provide more general constitutive assumptions to account for hydro-mechanical coupling.

Deformation of a granular porous medium is due to one of the following mechanisms or their combination:

(a) Deformation of grains
(b) The movement of grains

Based on a physical understating of soil mechanics and an intuitive view of underlying mechanisms, we submit that the deformation of the grains will result in a change in free energies of solid–fluid interfaces, while the grains movements, which is more significant, can result in a change in free energy of wetting-nonwetting (e.g., air–water) interfaces. The physical reasoning behind the latter statement is as follows. As the grains move, the pore sizes change, which in turn will cause a change in the curvature of the interface. Change of curvature goes along with a change in the free energy of the interface. For a detailed discussion on the curvature-dependent nature of free energies, see Eriksson and Ljunggren (1992), Gurtin and Jabbour (2002), and Chhapadia et al. (2011). This hydro-mechanical coupling can be captured by assuming that the free energy of interfaces depends on Lagrangian strain tensor of solid phase. Consequences of such assumption, the resulting stress tensor, and the physical interpretations of such dependency are presented in detail by Nikooee et al. (2012). Here, we assume a simpler constitutive assumption. We let the free energies of the interfaces depend on porosity (as an alternative measure for soil deformation). As explained above, for the case of rigid grains, the change in porosity produced by grains movements would mainly alter the free energy of fluid–fluid interfaces, and we do not consider free energies of solid–fluid interfaces to depend on porosity.

Hence, we consider the following forms of dependencies for free energies (assuming grains to be rigid, as is common in soil mechanics).

$$\begin{aligned} A^s &= A^s(\mathbf{E}^s, \theta^s, s^w) \\ A^\alpha &= A^\alpha(\rho^\alpha, \theta^\alpha, s^\alpha); \quad \alpha = w, n \\ A^{ws} &= A^{ws}(\Gamma^{ws}, \theta^{ws}, s^w, a^{ws}) \\ A^{ns} &= A^{ns}(\Gamma^{ns}, \theta^{ns}, s^w, a^{ns}) \\ A^{wn} &= A^{wn}(\Gamma^{wn}, \theta^{wn}, s^w, a^{wn}, \varepsilon) \end{aligned} \tag{16a–e}$$

where A denotes Helmholtz free energy function and $\mathbf{E}^s$ stands for Lagrangian strain tensor. Other constitutive assumptions are the same as in Hassanizadeh and Gray (1990). It is worth mentioning that, since density of rigid grains is constant, it is not included in the list of independent variables. Details on the selection of other dependencies and a proper method for selecting independent variables based on principles of continuum mechanics can be found in Hassanizadeh and Gray (1990) and Hassanizadeh (2003).

The next step is to combine balance equations and constitutive assumptions and impose the second law (the entropy inequality). Detailed mathematical manipulations for the case of rigid grains as well as deformable grains are presented in "Appendices A" and "B". The resulting formula for the effective stress tensor is described in the next section.

2.5 Exploitation of Entropy Inequality: Effective Stress Formula for Rigid Grains

As shown in "Appendix A," substitution of balance laws in the entropy inequality and then employing necessary auxiliary equations, lead to the following form for the effective stress tensor:

$$\mathbf{t}^e = \mathbf{t}^s - P^n\mathbf{I} + s^w P_c\mathbf{I} + k^{wn}a^{wn}\mathbf{I} \quad \text{where} \quad k^{wn} = -\frac{\partial A^{wn}}{\partial \varepsilon}\Gamma^{wn} \tag{17}$$

where $\mathbf{t}^e$ denotes effective stress tensor and k^{wn} is considered to be a material coefficient and $\mathbf{I}$ denotes the unit tensor. Note that in the definition of k^{wn}, the derivative of A^{wn} with respect to ε is taken with all other variables (namely Γ^{wn}, θ^{wn}, a^{wn}, and s^w) kept constant. This term accounts for changes in the contractile skin forces as a result of change in the curvature of interfaces (due to movement of grains).

As porosity decreases, the curvature of the fluid–fluid interfaces increase and thus, the interfacial free energy increases. Therefore, we expect k^{wn} to be positive. Also, in general, k^{wn} can depend on state variables such as temperature, porosity, and saturation. However, in the absence of experimental data, it is not yet possible to discuss the physical dependency and the magnitude of this coefficient for different soil types and soil textures. Further research and more information on the values of specific interfacial area and suction stress are required to shed light on the values of this coefficient.

In arriving at Eq. 17, we have assumed that local thermal equilibrium conditions exist. That is, at a macroscopic point, the temperature of different phases and interfaces is the same.

These assumptions are commonly reasonable in unsaturated soil mechanics practice. However, they can be revoked for other cases of interest, as shown in "Appendix B."

The closest study in the literature which arrives at the equation of effective stress accounting for interfacial contribution is that of Coussy and Dangla (2002). However, they have made a number of simplifying assumptions. In particular, they have considered interfaces without mass and no balance laws for interfaces has been considered. The effects of interfaces on the macroscopic behavior have exclusively been accounted for in the solid skeleton free energy. In the approach employed here, no explicit formulations for macroscopic free energy functions of a phase or interface introduced. Instead, general dependence of free energy of different constituents is postulated in which change of curvature of interfaces and their redistribution due to grain movement were accounted for. Moreover, we do not consider interfaces to be massless and balance laws for interfaces as well as phases were introduced.

3 Results and Discussion

3.1 The Concept of SSCS

The effective stress formulation accounts for the fact that the presence of fluid(s) in soil modifies the state of stress inside the soil medium. Such effects are represented by the last three terms in Eq. 17. The last two terms account for capillary forces and interfacial effects. It is known that as a dry soil is wetted, an extra force among soil grains comes into existence,

due to capillary effects. These extra forces have been referred to as suction stress (Lu and Likos 2006). In our formulations, Suction stress (SS) is represented by the last two terms in Eq. 17

$$\mathrm{SS} = s^w P_c + k^{wn} a^{wn}. \tag{18}$$

It is known that even if there is no (significant) change in saturation, there could still be a significant change in the effective stress (see e.g. Khalili and Zargarbashi 2010). This occurs especially along scanning curves, where saturation is almost constant but P_c and a^{wn} may change. Our proposed equation for suction stress accounts for changes in the effective stress along scanning curves as it is a function of saturation, capillary pressure, and specific interfacial area. However, only two of these state variables are known to be independent (Hassanizadeh and Gray 1993).

In order to implement Eqs. 17 or 18, we need to know the amount of air–water interfacial area, a^{wn}. In principle, the required relationship should be obtained from experiments. In the absence of such experimental results, we employ a formula that has been recently obtained from pore-network modeling studies by Joekar-Niasar et al. (2008). The equation reads:

$$a^{wn}(P_c, s^w) = c_{00} + c_{01}(s^w) + c_{10}(P_c) + c_{11}(s^w \cdot P_c) + c_{02}(s^w)^2 + c_{20}(P_c)^2 \tag{19}$$

where c_{ij} $(i, j = 0, 1, 2)$ are constants.

Hereafter, we assume k^{wn} to be constant and a material coefficient. Then substitution of Eq. 19 in the suction stress formula, Eq. 18, yields:

$$\mathrm{SS}(P_C, s^w) = C_{00} + C_{01}(s^w) + C_{10}(P_c) + C_{11}(s^w \cdot P_c) + C_{02}(s^w)^2 + C_{20}(P_c)^2 \tag{20}$$

where $C_{ij}; i, j = 0, 1, 2$ are constants. This bi-quadratic relationship (or any other analogous relation) is expected to be a property of the porous medium. It forms a three-dimensional surface to which we refer as the SSCS. It is expected to be a unique surface that gives values of suction stress for different states of matric suction and saturation. The scope of application and the capability of the proposed suction stress surface to model experimental results are examined in Sect. 3.3.

One should note that Eq. 18 can be simplified for a saturated soil just before the start of desaturation. Desaturation mainly starts when the value of capillary pressure surpasses the air entry value, $P_{c,\mathrm{ae}}$. Before that (i.e., $P_c < P_{c,\mathrm{ae}}$) saturation is unity and there are no air–water interfaces. Therefore, Eq. 18 may be simplified to $\mathrm{SS} = P_c$. Also in the wetting branch after the air expulsion value (as soon as air phase becomes disconnected), we assume that the contribution of air–water interfaces becomes negligible and we let the suction stress to be equal to capillary pressure.

With these considerations, the following equation for SS can be given:

$$\mathrm{SS}(P_C, s^w) = \begin{cases} P_c & P_c \le P_{c,e} \\ C_{00} + C_{01}(s^w) + C_{10}(P_c) + C_{11}(s^w \cdot P_c) + C_{02}(s^w)^2 + C_{20}(P_c)^2 & \textit{elsewhere} \end{cases} \tag{21}$$

where $P_{c,e}$ is the air entry or air expulsion value for drying and wetting branches, respectively. A 2D illustration of this equation is shown in Fig. 1, which may be seen as a projection of the suction stress surface on the SS-P_c plane. As shown in this figure, suction stress value is bounded between drying and wetting paths. All points between these two curves can be considered as possible states that a soil can experience. Before the air entry and air expulsion values, suction stress lies on line $SS = P_c$, as shown in Fig. 1. For all other points on drying, wetting, or scanning curves, the corresponding suction stress can be calculated from Eq. 20 provided that P_c and s^w are known.

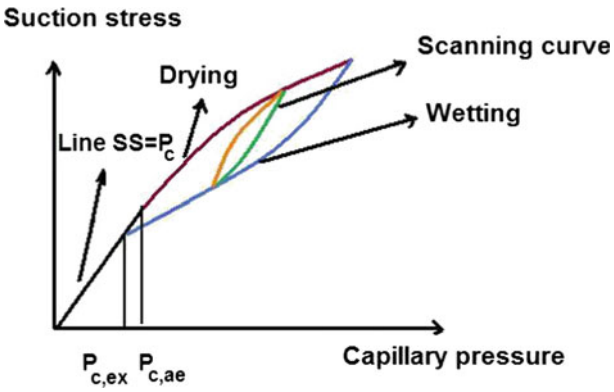

Fig. 1 A schematic sketch of suction stress 2D trajectories

3.2 Bishop's Effective Stress Parameter

The proposed equation for the effective stress tensor is a non-Bishop type equation as it also includes a third term which accounts for interfacial effects. However, one may still be interested to determine its equivalent Bishop's type equation and the corresponding effective stress parameter. In analogy with Eq. 1, Eq. 17 can be rewritten in the following form:

$$\sigma'_{ij} = (\sigma_{ij} - P^a \delta_{ij}) + \chi \; P_c \delta_{ij}$$
$$where: \quad \chi = s^w + \frac{k^{wn} a^{wn}}{P_c} \tag{22}$$

The amount of specific air–water interfacial area can be calculated from the area between soil water retention curve (SWRC) and the saturation axis (Grant and Gerhard 2007). Therefore, Eq. 22 can be transformed into the following relationship:

$$\chi = s^w + K \left(\int_{s^w=1}^{s^w} P_c \mathrm{d}s^w \right) / P_c \tag{23}$$

where K can be a function of degree of saturation, capillary pressure, and porosity and can also be dependent on soil type (grain shapes, grain surface roughness); see "Appendix C" for more details.

Alternatively, one can also relate the suction stress and the effective stress parameter as follows:

$$\chi = \begin{cases} 1 & P_c \le P_{c,e} \\ \frac{SS}{P_c} & elsewhere \end{cases} \tag{24}$$

These equations are hereafter compared with relationships available in the literature. For this purpose, current relationships for the effective stress parameter, χ, are classified in five categories as presented in Table 1.

While our results prescribe the effective stress parameter to be a function of both P_c and s^w, categories (1) and (2) in Table 1 suggest a dependence of χ on either s^w or P_c. But, then one needs to prescribe different values for parameters of such formulations to determine the effective stress parameter for different hydraulic paths, as χ is known to be hysteretic (Khalili and Zargarbashi 2010).

Table 1 Various relationships for effective stress parameter, χ

Category	χ expressed as a function of:	Example†	Ref.
(1)	$\chi = f(S^w)$	$\chi = S^w$	Nuth and Laloui (2008a), Schrefler (1984)
		$\chi = \left(S^w - S_m^w\right) / \left(1 - S_m^w\right)$	Alonso et al. (2010)
		$\chi = \left(S^w - S_0^w\right) / \left(1 - S_0^w\right)$	Lu et al. (2010)
(2)	$\chi = f(P_c)$	$\chi = 1 \quad P_c \le P_{c,ae}$ $\chi = \left(P_c / P_{c,ae}\right)^{-\gamma} \quad P_c > P_{c,ae}$	Khalili and Khabbaz (1998)
		$\chi = 1 \quad P_c \le P_{c,e}$ $\chi = \left(P_c / P_{c,e}\right)^{-\gamma *} \quad P_c > P_{c,e}$	Khalili and Zargarbashi (2010)
		$\chi = \left(P_{c,r} / P_{c,e}\right)^{-\gamma} \left(P_c / P_{c,r}\right)^{\xi **}$	
(3)	$\chi = f(a^{ws})$	$\chi = x^{ws} = a^{ws} / a^s$	Gray and Schrefler (2001)
(4)	$\chi = f(a^{ws}, S^w)$	$\chi = (1 - \varepsilon) x^{ws} + \varepsilon S^{w***}$	Gray et al. (2009)
(5)	$\chi = f(S^w, P_c)$	$\chi = S^w + (2/3) \left[\int P_c d(s^w)\right] / P_c$	Coussy and Dangla (2002)

† S_m^w: degree of saturation of micro-structure; S_0^w : residual degree of saturation; γ: material parameter; x^{ws}: wetted fraction of grains; a^s: total solid (grains) area in an REV; $P_{c,r}$: the point of suction reversal for scanning curves; ζ: material parameter

* For drying and wetting branch. ** For scanning branch. *** For compressible grains

Table 2 Coefficients of SWRC for different soil samples used in this study

Soil type*	Path**	Fitting parameters					
		a'	m	n	Z ($\times 10^{-3}$)	U ($\times 10^{-1}$)	Y
(1)	D	0.65	0.05	4.33	–	–	–
	S	–	–	–	−0.45	9.75	0.91
	W	0.64	0.02	255.16	–	–	–
(2)	D	0.54	0.86	1.75	–	–	–
	S	–	–	–	4944	–0.05	–4.55
	W	0.37	0.23	41.81	–	–	–
(3)	D	4.06	4.54	2.63	–	–	–
	S	–	–	–	0.02	66.17	0.50
	W	0.23	0.26	6.59	–	–	–
(4)	D	0.07	0.32	12.21	–	–	–
	S	–	–	–	–3412	0.04	3.76
	W	0.05	0.24	33.81	–	–	–
(5)	D	1.16	0.09	2.92	–	–	–
	S	–	–	–	237	–0.03	0.68
	W	0.53	0.14	1.05	–	–	–

* Soil types: (1) = Buffalo Dam clay, (2) = Bourke silt, (3) = Mixture of Sydney sand and kaolin, (4) = Mixture of Sydney sand and Buffalo Dam clay, (5) = Compacted kaolin samples

** *D* drying, *W* wetting, *S* scanning

The 3rd and 4th category equations assume a dependence of the effective stress parameter on the wetted fraction of grains and/or saturation. But, Culligan et al. (2006) have shown that the wetted fraction of grains does not have a hysteretic behavior, whereas the effective stress

Table 3 Coefficients of SSCS

Soil type	Coefficients of SSCS					
	C_{02} (kPa)	C_{20} (kPa^{-1}) ($\times 10^{-3}$)	C_{11}	C_{10}	C_{01} (kPa)	C_{00} (kPa)
(1)	16,227	3.80	25.19	−24	−32612	16,373
(2)	570	0.94	3.09	−1.24	−851	279
(3)	626	2.30	2.30	−1.51	−1094	483
(4)	166	14.20	14.23	−5.54	−246	68
(5)	6,153	2.02	11.43	−10.71	−12,325	6,187

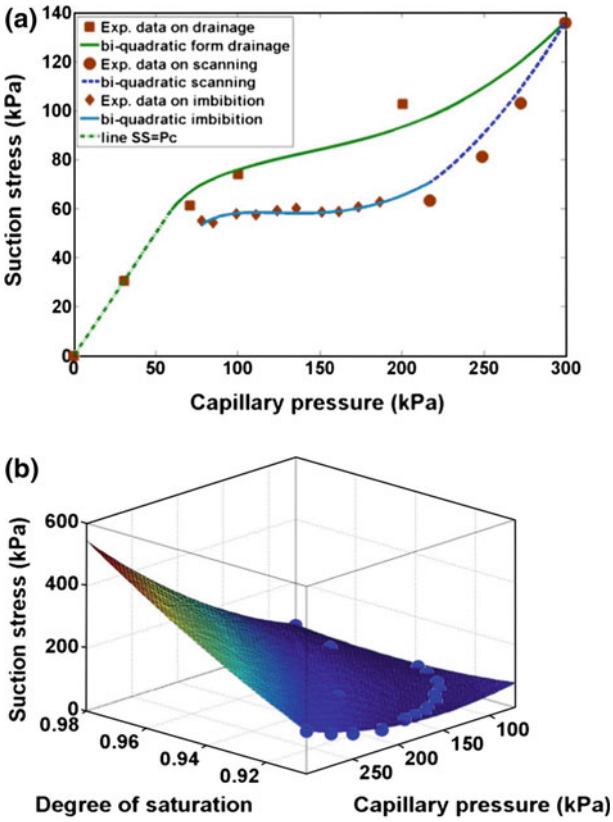

Fig. 2 **a** 2D plot (drying and wetting trajectories) and **b** 3Dplot (surface) of suction stress for Buffalo dam clay (Exp. data from Khalili and Zargarbashi 2010)

parameter shows a marked hysteretic behavior (Khalili and Zargarbashi 2010). Of course, a dependence on the grains wetted fraction (or on the solid–fluid specific interfacial area) may be needed when grains are deformable (see "Appendix B").

In category 5, we have the equation suggested by Coussy and Dangla (2002). It can be obtained from Eq. 23 by setting K equal to 2/3. Since K can be dependent on suction and degree of saturation, the application of this relationship needs further research especially for

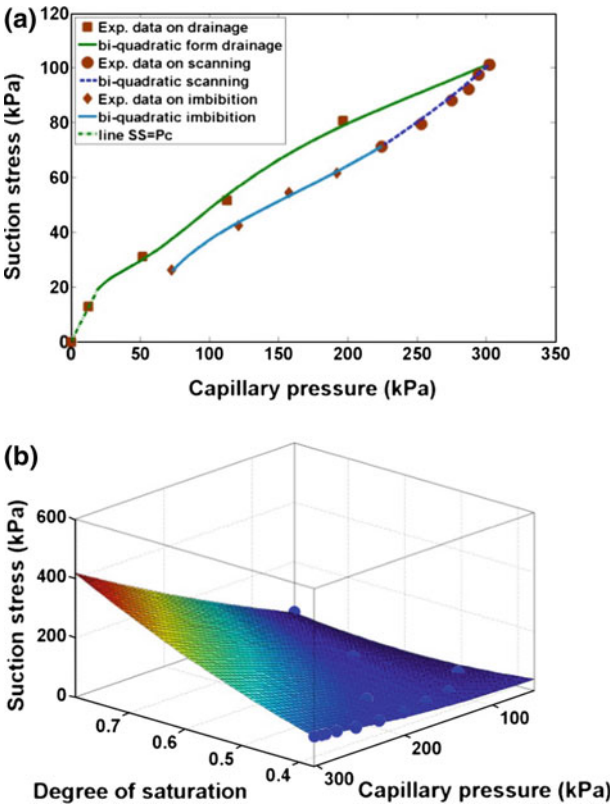

Fig. 3 **a** 2D plot (drying and wetting trajectories) and **b** 3Dplot (surface) of suction stress for Bourke silt (Exp. data from Khalili and Zargarbashi 2010)

a complete hydraulic cycle. In this study, the accuracy and efficiency of Eq. 24 has been investigated whereas Eq. 23 has been discussed in details elsewhere (Nikooee 2012).

In fact, in order to express resulting equation based on the area under capillary pressure–saturation curve (soil water retention curve), one should also consider the energy which is dissipated to heat when water flows through porous channels, for which additional coefficients are needed which are not constant in general. Moreover, two separate formulae which give the variation of the interfacial contribution on each hydraulic branch are needed when dealing with drying and wetting paths. These issues and further details are introduced in "Appendix C".

3.3 Verification of the Proposed Relationships

The experimental results of Khalili and Zargarbashi (2010) as well as those of Uchaipichat (2010a,b) were employed to investigate the utility of Eq. 21 for suction stress surface. Their results include variation of the effective stress parameter at various states of matric suction during wetting, drying, and scanning cycles.

Khalili and Zargarbashi (2010) performed multi-stage drying and wetting shear tests on four laboratory-compacted soils: a low plasticity clay from Buffalo Dam in Victoria,

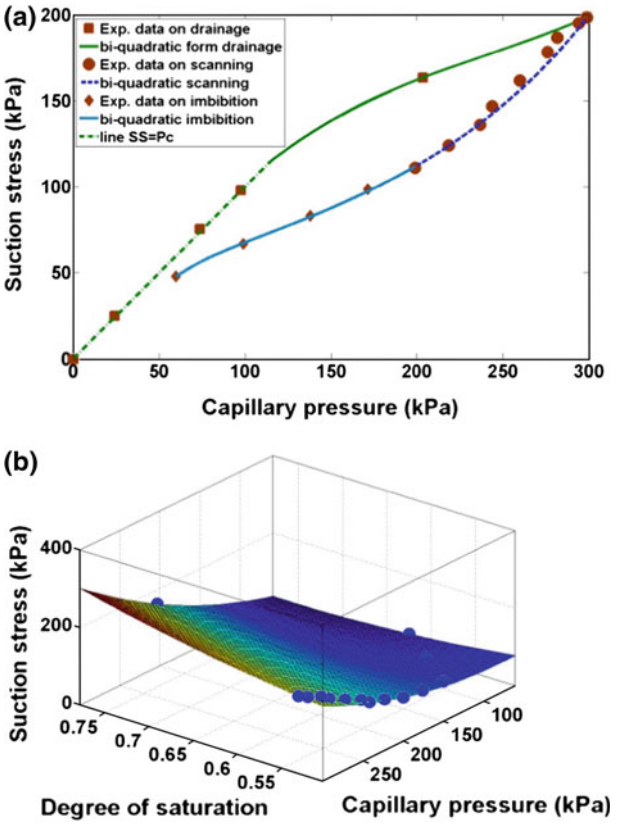

Fig. 4 **a** 2D plot (drying and wetting trajectories) and **b** 3Dplot (surface) of suction stress for mixture of Sydney sand (75 %) and kaolin (25 %) (Exp. data from Khalili and Zargarbashi 2010)

Australia; a mixture of Sydney sand (70 %) and Buffalo clay (30 %); a low plasticity silt from the Bourke region of New South Wales, Australia; and a mixture of Sydney sand (75 %) and Kaolin (25 %). Basic properties of the soil samples and details of their experiments including the followed stress path can be found in Khalili and Zargarbashi (2010). They obtained values of the effective stress parameter as well as the soil water retention data in drying, scanning, and wetting paths for the four soil samples.

Uchaipichat (2010a,b) performed triaxial tests on unsaturated compacted kaolin samples, following both drying and wetting paths. Details of his experiment can be found in Uchaipichat (2010a,b) and variation of the effective stress parameter as obtained from those experiments are presented in Uchaipichat (2010b).

Our approach for verification of Eq. 21 was to fit it to the drying and wetting data and determine coefficients C_{ij} for the five different soil samples. Subsequently, it was used to predict the scanning data. The soil water retention relationship proposed by Fredlund and Xing (1994) was employed for main drying and wetting branches:

$$s^w = \frac{1}{\left\{\ln\left[\exp(1) + \left(\frac{P_c}{a' P_0}\right)^n\right]\right\}^m} \tag{25}$$

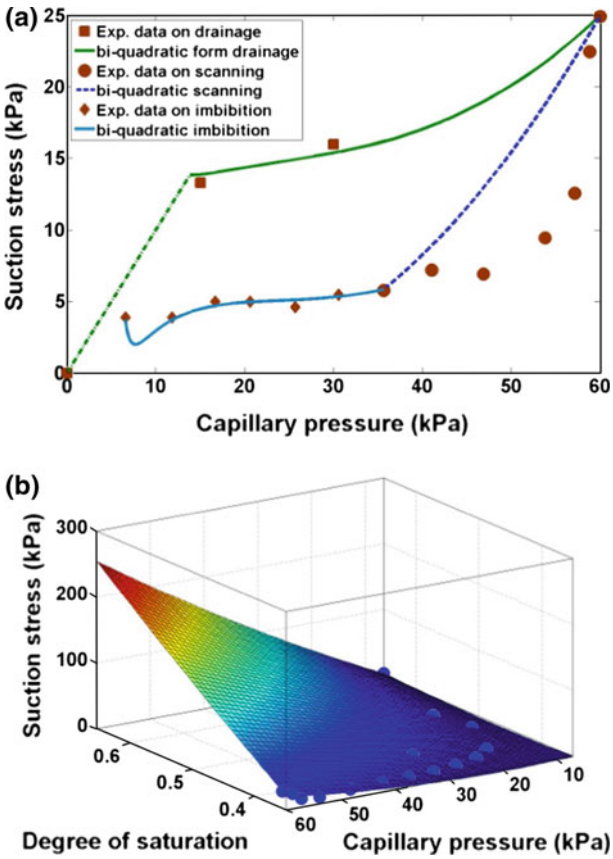

Fig. 5 **a** 2D plot (drying and wetting trajectories) and **b** 3Dplot (surface) of suction stress for mixture of Sydney sand (70 %) and Buffalo dam clay (30 %) (Exp. data from Khalili and Zargarbashi 2010)

where P_0 is a reference pressure, which we have set equal to the atmospheric pressure at sea level (101 kPa). Coefficients m, n, and a' were determined by fitting this equation to the experimental data. This was done for drying and wetting branches of each soil separately.

To express soil water retention data at scanning curves, power law relationships can be used (Khalili et al. 2008). In this study, the following relationship was used:

$$s^w = Z\left(\frac{P_c}{P_0}\right)^U + Y \tag{26}$$

Values of coefficients a', m, n, Z, U, and Y for the five soil types are given in Table 2. In all tables, the values of coefficients are dimensionless unless otherwise stated.

For the regression of the drying and wetting branches of SWRC, an enhanced least square method was used. The coefficient m specifies the position of the tail of the curve (Fredlund and Xing 1994). Therefore, first, the coefficient m was found such that the fitted curve could go through the ending part of experimental data points (the last data points on drying and wetting branches). Next, a constrained least square method was used to find the best values of a' and n. Method of Lagrangian multiplier was used to ensure the fitted curve follows experimental

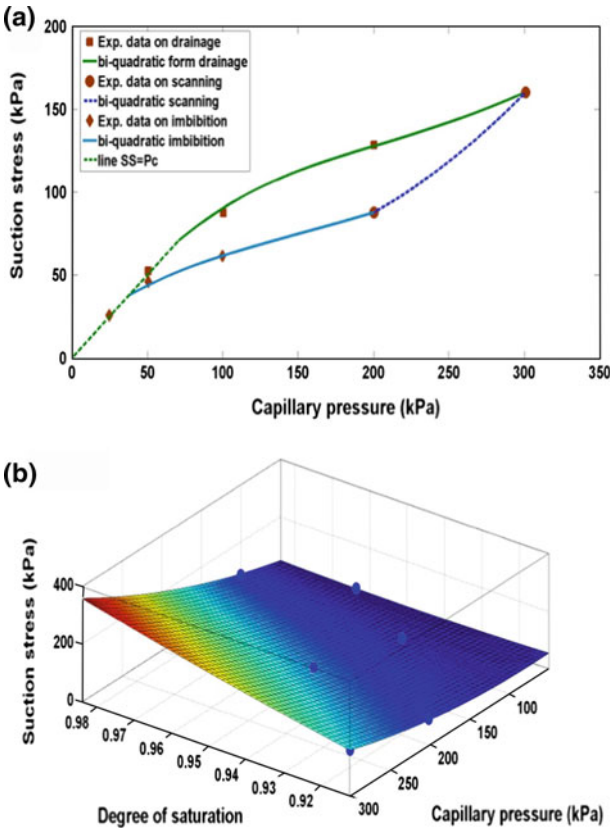

Fig. 6 **a** 2D plot (drying and wetting trajectories) and **b** 3Dplot (surface) of suction stress for compacted kaolin samples (Exp. data from Uchaipichat 2010b)

suction values, as much as possible, at reversal points where drying and wetting curves join the scanning path.

For the scanning curve, first, the coefficient U was found from the regression. Then, the fitting coefficients Y and Z were adjusted such that the scanning curve could also pass through the two suction reversal points. This procedure allows the SWRC equations to be continuous at the suction reversal points.

Finally, the data points of effective stress parameter at various capillary pressure levels along with the corresponding SWRCs were used to calibrate the model. Values of coefficients C_{ij} of the SSCS (Eq. 21) were obtained by fitting drying and wetting data points. Resulting values are given in Table 3. The 2D plots and 3D plots of the suction stress determined from model calibration are presented in Figs. 2, 3, 4, 5, and 6 for the five different soils.

It is clear that the suction stress surface fits the drying and wetting data fairly well. Furthermore, the resulting surface is capable of predicting the data for the scanning branch with a reasonable accuracy (note that the scanning data were not used in the fitting process). Only for soil type (4), which was a mixture of Buffalo Dam clay and Sydney sand, the agreement between our proposed equation and data is poor. This is perhaps due to the clay type. Since sample (3) had almost the same proportions of sand and clay as soil type (4) but different clay type (Kaolinite). As shown in Fig. 6, the model is in good agreement

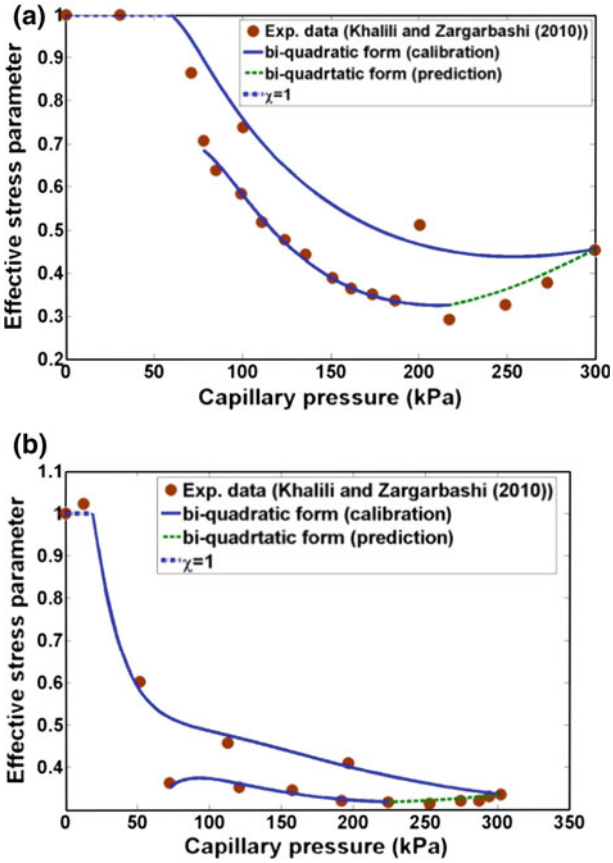

Fig. 7 Plots of effective stress parameter **a** Buffalo dam clay and **b** Bourke silt

with data of Uchaipichat (2010c) noting that these data belong to compacted kaolin samples and therefore, confirming the hypothesis that texture and clay type may play an important role.

Plots of the effective stress parameter χ, as obtained from Eq. 24, versus experimental data are depicted in Figs. 7, 8, and 9. Experimental data reveal that the effective stress parameter decreases considerably for the wetting scanning curves whereas the degree of saturation is nearly constant. This behavior is captured very well with our proposed equation as χ depends not only on saturation but also on capillary pressure. Indeed, Eq. 22 shows that even if the change in the saturation is negligible, the effective stress parameter can still change because of the term associated with the interfacial energy. This term includes the amount of specific air–water interfacial area as well as capillary pressure. This indicates that the effective stress parameter is neither equal to the degree of saturation nor is a sole function of degree of saturation. It has to depend on capillary pressure as well, to reproduce observed experimental trends. The proposed equations for the SSCS and effective stress parameter have this unique feature. It is only when the interfacial effects are negligible that the effective stress parameter may be considered as an exclusive function of the degree of saturation.

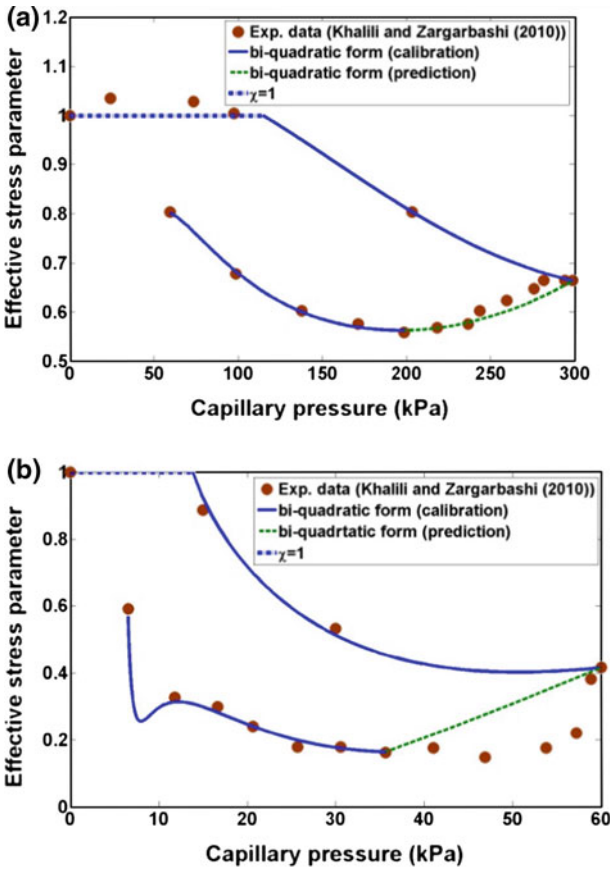

Fig. 8 Plots of effective stress parameter **a** mixture of Sydney sand (75 %) and kaolin (25 %). **b** Mixture of Sydney sand (70 %) and Buffalo dam clay (30 %)

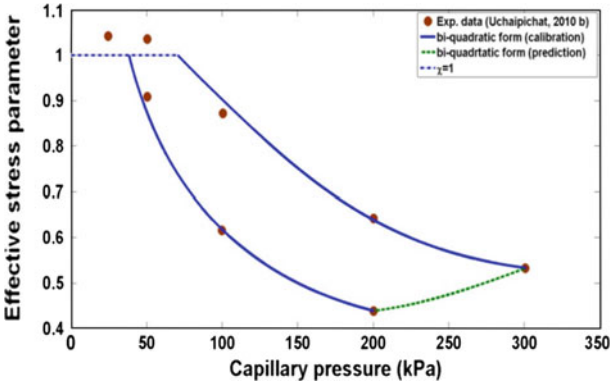

Fig. 9 Plot of effective stress parameter for compacted kaolin samples

4 Concluding Remarks

Four major contributions of this study can be summarized as follows:

1. A rational thermodynamic framework was used in which hydro-mechanical coupling was introduced through appropriate constitutive assumptions. This led to a new equation for the effective stress in which interfacial energy plays a role and can include phenomena such as bonding effects and the variation of effective stress within a full hydraulic cycle.
2. Examination of the proposed equation shows that the sharp decrease in the values of effective stress parameter during wetting scanning curves, observed in experimental studies, can be attributed to the change in the fluid–fluid interfacial areas (their redistribution and variation in their amount). In other words, it was shown that the air–water specific interfacial area must be included in the formulation for a complete description of the effective stress. The role of air–water interfacial energy on the effective stress can be markedly traced in the values of effective stress parameter when a slight change in the degree of saturation is accompanied by a considerable change in the values of effective stress parameter.
3. Based on the proposed form for the effective stress tensor, and expressing the air–water specific area as a function of matric suction and saturation, the concept of SSCS was introduced, for which a bi-quadratic form was presented.
4. The proposed bi-quadratic surface was employed to describe the variation of suction stress for a full hydraulic cycle. This was done by simulating a set of available data found in the literature.

Of course, further research is needed to explore comprehensively the adequacy of the proposed equation and to obtain the most suitable form of SSCS for different soil types and various soil textures.

Finally, two main future research directions can also be suggested. First, one should experimentally and theoretically explore the variation of effective stress, as well as suction stress, within full hydraulic cycles and for different soils, to arrive at the most suitable form for SSCS. Second, special apparatus needs to be designed to determine values of air–water specific interfacial area while changes in other hydraulic as well as mechanical state variables are monitored. Further research on transient conditions can also be sought where evolution of interfaces plays an important role. This will augment our current knowledge on the role of interfacial areas on hydro-mechanical coupling in unsaturated soils.

Acknowledgments The first author and SMH are members of the International Research Training Group NUPUS, financed by the German Research Foundation (DFG) and The Netherlands Organization for Scientific Research (NWO). EN wishes to express his sincere gratitude to the Environmental Hydrogeology Group of Utrecht University (UU) for their spiritual, intellectual and financial support during his stay in UU. The authors gratefully acknowledge constructive comments of the reviewers.

Appendix A: Exploitation of Entropy Inequality for a Granular Porous Medium with Rigid Grains

Starting from the expansion of the material derivatives and applying the chain rule of differentiation to Eqs. (16a–e), we get:

$$\frac{\mathrm{D}^w A^w}{\mathrm{D}t} = \frac{\partial A^w}{\partial \rho^w}\frac{\mathrm{D}^w \rho^w}{\mathrm{D}t} + \frac{\partial A^w}{\partial s^w}\frac{\mathrm{D}^w s^w}{\mathrm{D}t} + \frac{\partial A^w}{\partial \theta^w}\frac{\mathrm{D}^w \theta^w}{\mathrm{D}t}$$

$$\frac{\mathrm{D}^{wn} A^{wn}}{\mathrm{D}t} = \frac{\partial A^{wn}}{\partial \Gamma^{wn}}\frac{\mathrm{D}^{wn} \Gamma^{wn}}{\mathrm{D}t} + \frac{\partial A^{wn}}{\partial s^w}\frac{\mathrm{D}^{wn} s^w}{\mathrm{D}t} + \frac{\partial A^{wn}}{\partial \theta^{wn}}\frac{\mathrm{D}^{wn} \theta^{wn}}{\mathrm{D}t} + \frac{\partial A^{wn}}{\partial a^{wn}}\frac{\mathrm{D}^{wn} a^{wn}}{\mathrm{D}t}$$

$$
\begin{aligned}
&\qquad\qquad + \frac{\partial A^{wn}}{\partial \varepsilon}\frac{\mathrm{D}^{wn}\varepsilon}{\mathrm{D}t}\\
\frac{\mathrm{D}^{ws}A^{ws}}{\mathrm{D}t} &= \frac{\partial A^{ws}}{\partial \Gamma^{ws}}\frac{\mathrm{D}^{ws}\Gamma^{ws}}{\mathrm{D}t} + \frac{\partial A^{ws}}{\partial s^{w}}\frac{\mathrm{D}^{ws}s^{w}}{\mathrm{D}t} + \frac{\partial A^{ws}}{\partial \theta^{ws}}\frac{\mathrm{D}^{ws}\theta^{ws}}{\mathrm{D}t} + \frac{\partial A^{ws}}{\partial a^{ws}}\frac{\mathrm{D}^{ws}a^{ws}}{\mathrm{D}t}\\
\frac{\mathrm{D}^{ns}A^{ns}}{\mathrm{D}t} &= \frac{\partial A^{ns}}{\partial \Gamma^{ns}}\frac{\mathrm{D}^{ns}\Gamma^{ns}}{\mathrm{D}t} + \frac{\partial A^{ns}}{\partial s^{w}}\frac{\mathrm{D}^{ns}s^{w}}{\mathrm{D}t} + \frac{\partial A^{ns}}{\partial \theta^{ns}}\frac{\mathrm{D}^{ns}\theta^{ns}}{\mathrm{D}t} + \frac{\partial A^{ns}}{\partial a^{ns}}\frac{\mathrm{D}^{ns}a^{ns}}{\mathrm{D}t}\\
\frac{\mathrm{D}^{s}A^{s}}{\mathrm{D}t} &= \frac{\partial A^{s}}{\partial \mathbf{E}^{s}} : \frac{\mathrm{D}^{s}\mathbf{E}^{s}}{\mathrm{D}t} + \frac{\partial A^{s}}{\partial s^{w}}\frac{\mathrm{D}^{s}s^{w}}{\mathrm{D}t} + \frac{\partial A^{s}}{\partial \theta^{s}}\frac{\mathrm{D}^{s}\theta^{s}}{\mathrm{D}t}\\
\frac{\mathrm{D}^{n}A^{n}}{\mathrm{D}t} &= \frac{\partial A^{n}}{\partial \rho^{n}}\frac{\mathrm{D}^{n}\rho^{n}}{\mathrm{D}t} + \frac{\partial A^{n}}{\partial s^{n}}\frac{\mathrm{D}^{n}s^{n}}{\mathrm{D}t} + \frac{\partial A^{n}}{\partial \theta^{n}}\frac{\mathrm{D}^{n}\theta^{n}}{\mathrm{D}t}
\end{aligned}
\tag{A-1}
$$

The terms $\mathrm{D}\rho^{\alpha}/\mathrm{D}t$ & $\mathrm{D}^{\alpha\beta}\Gamma^{\alpha\beta}/\mathrm{D}t$ will be eliminated from above equations by means of mass balance equations. These are recast in the following form:

$$
\begin{aligned}
\frac{\mathrm{D}^{\alpha}\rho^{\alpha}}{\mathrm{D}t} &= \frac{\hat{e}^{\alpha}_{\alpha\beta} + \hat{e}^{\alpha}_{\alpha\gamma}}{\varepsilon s^{\alpha}} - \rho^{\alpha}(\nabla.\mathbf{v}^{\alpha}) - \frac{\mathrm{D}^{\alpha}(\varepsilon s^{\alpha})}{\mathrm{D}t}\frac{\rho^{\alpha}}{\varepsilon^{\alpha}} \quad \alpha = w, n \& \beta, \gamma \neq \alpha\\
\frac{\mathrm{D}^{\alpha\beta}\Gamma^{\alpha\beta}}{\mathrm{D}t} &= \left[-\Gamma^{\alpha\beta}\left(\frac{\mathrm{D}^{\alpha\beta}a^{\alpha\beta}}{\mathrm{D}t}\right) + \hat{e}^{\alpha\beta}_{\alpha\beta\gamma} - \hat{e}^{\alpha}_{\alpha\beta} - \hat{e}^{\beta}_{\alpha\beta} - \Gamma^{\alpha\beta}a^{\alpha\beta}\left(\nabla.\mathbf{w}^{\alpha\beta}\right)\right]\frac{1}{a^{\alpha\beta}}\\
\frac{\mathrm{D}^{s}\rho^{s}}{\mathrm{D}t} &= \frac{\hat{e}^{s}_{ns} + \hat{e}^{s}_{ws}}{1-\varepsilon} - \rho^{s}(\nabla.\mathbf{v}^{s}) - \frac{\mathrm{D}^{s}(1-\varepsilon)}{\mathrm{D}t}\frac{\rho^{s}}{1-\varepsilon} = 0 \ (\textit{rigid grains})
\end{aligned}
\tag{A-2}
$$

Combination of equations (8)–(11), (14)–(15) and (A-1) and (A-2) and substitution in the entropy inequality (13) results in a general entropy inequality for a multiphase system, (see Hassanizadeh and Gray 1990, for details of a similar procedure):

$$
\begin{aligned}
\sum \Lambda^{\alpha} + \Lambda^{\alpha\beta} = &-\sum_{\alpha}\frac{\varepsilon^{\alpha}\rho^{\alpha}}{\theta^{\alpha}}\frac{\mathrm{D}^{\alpha}\theta^{\alpha}}{\mathrm{D}t}\left\{\eta^{\alpha} + \frac{\partial A^{\alpha}}{\partial \theta^{\alpha}}\right\} - \sum_{\alpha\beta}\frac{a^{\alpha\beta}\Gamma^{\alpha\beta}}{\theta^{\alpha\beta}}\frac{\mathrm{D}^{\alpha\beta}\theta^{\alpha\beta}}{\mathrm{D}t}\left\{\eta^{\alpha\beta} + \frac{\partial A^{\alpha\beta}}{\partial \theta^{\alpha\beta}}\right\}\\
&+ \sum_{\alpha\neq s}\frac{\mathbf{d}^{\alpha}}{\theta^{\alpha}} : \left\{\varepsilon s^{\alpha}\left(p^{\alpha}\mathbf{I} + \mathbf{t}^{\alpha}\right)\right\}\\
&+ \frac{(1-\varepsilon)}{\theta^{s}}\mathbf{d}^{s} : \left\{-\rho^{s}(Grad\mathbf{F}^{s})^{T}\cdot\frac{\partial A^{s}}{\partial \mathbf{E}^{s}}\cdot(Grad\mathbf{F}^{s}) + p^{s}\mathbf{I} + \mathbf{t}^{s}\right.\\
&\left. - \frac{a^{wn}\Gamma^{wn}\theta^{s}}{\theta^{wn}}\left(\frac{\partial A^{wn}}{\partial \varepsilon}\right)\mathbf{I}\right\} + \dot{\varepsilon}\left[\frac{s^{n}p^{n}}{\theta^{n}} + \frac{s^{w}p^{w}}{\theta^{w}} - \frac{p^{s}}{\theta^{s}}\right]\\
&+ \sum_{\alpha}\mathbf{v}^{\alpha,s}\cdot\frac{1}{\theta^{\alpha}}\left[p^{\alpha}\nabla(\varepsilon s^{\alpha}) - \varepsilon s^{\alpha}\rho^{\alpha}\frac{\partial A^{\alpha}}{\partial s^{\alpha}}\nabla(s^{\alpha}) - \sum_{\alpha\neq\beta}\hat{\mathbf{T}}^{\alpha}_{\alpha\beta}\right.\\
&\left. + \sum_{\alpha\neq\beta}\hat{\mathbf{T}}^{\alpha}_{\alpha\beta}\frac{\theta^{\alpha\beta,\alpha}}{\theta^{\alpha\beta}}\right] + \sum_{\alpha\beta}\frac{1}{\theta^{\alpha\beta}}\mathbf{w}^{\alpha\beta,s}\cdot\left[-a^{\alpha\beta}\Gamma^{\alpha\beta}\left(\frac{\partial A^{\alpha\beta}}{\partial s^{w}}\right)\nabla(s^{w})\right.\\
&-\nabla(a^{\alpha\beta})\left(\gamma^{\alpha\beta} + a^{\alpha\beta}\Gamma^{\alpha\beta}\frac{\partial A^{\alpha\beta}}{\partial a^{\alpha\beta}}\right) + \hat{\mathbf{T}}^{\alpha}_{\alpha\beta} + \hat{\mathbf{T}}^{\beta}_{\alpha\beta} - \hat{\mathbf{S}}^{\alpha\beta}_{\alpha\beta\gamma}\\
&\left.-\hat{\mathbf{S}}^{\alpha\beta}_{\alpha\beta\gamma}\frac{\theta^{\alpha\beta,s}}{\theta^{s}}\right] + \frac{1}{\theta^{wn}}\mathbf{w}^{wn,\,s}\cdot\left(-a^{wn}\Gamma^{wn}\left(\frac{\partial A^{wn}}{\partial \varepsilon}\right)\nabla(\varepsilon)\right)\\
&-\left(\frac{a^{wn}\Gamma^{wn}}{\theta^{wn}}\right)\left(\frac{\partial A^{wn}}{\partial \varepsilon}\right)\left(\frac{\hat{e}^{s}_{ns} + \hat{e}^{s}_{ws}}{\rho^{s}}\right)\\
&+\dot{s}^{w}\left[\frac{\varepsilon p^{w}}{\theta^{w}} - \frac{\varepsilon p^{n}}{\theta^{n}} - \frac{\varepsilon s^{w}\rho^{w}}{\theta^{w}}\frac{\partial A^{w}}{\partial s^{w}} + \frac{\varepsilon s^{n}\rho^{n}}{\theta^{n}}\frac{\partial A^{n}}{\partial s^{n}} - \frac{(1-\varepsilon)\rho^{s}}{\theta^{s}}\frac{\partial A^{s}}{\partial s^{w}}\right.
\end{aligned}
$$

$$
\begin{aligned}
&- \sum_{\alpha\beta} \frac{\Gamma^{\alpha\beta} a^{\alpha\beta}}{\theta^{\alpha\beta}} \left(\frac{\partial A^{\alpha\beta}}{\partial s^w} \right) \Bigg] \\
&+ \sum_{\alpha\beta} \frac{1}{\theta^{\alpha\beta}} \mathbf{d}^{\alpha\beta} : \left\{ a^{\alpha\beta} (\mathbf{s}^{\alpha\beta} - \gamma^{\alpha\beta} \mathbf{I}) \right\} - \frac{\dot{a}^{wn}}{\theta^{wn}} \left[a^{wn} \Gamma^{wn} \frac{\partial A^{wn}}{\partial a^{wn}} + \gamma^{wn} \right] \\
&- \sum_{\alpha\beta = ws, ns} \frac{\dot{a}^{\alpha\beta}}{\theta^{\alpha\beta}} \left[a^{\alpha\beta} \Gamma^{\alpha\beta} \frac{\partial A^{\alpha\beta}}{\partial a^{\alpha\beta}} + \gamma^{\alpha\beta} + \frac{\theta^{\alpha\beta} (1-\varepsilon) \rho^s}{\theta^s} \frac{\partial A^s}{\partial a^{\alpha\beta}} \right] \\
&+ \sum_{\alpha} \nabla \theta^{\alpha} \cdot \frac{\varepsilon^{\alpha} \mathbf{q}^{\alpha}}{(\theta^{\alpha})^2} + \sum_{\alpha\beta} \nabla \theta^{\alpha\beta} \cdot \frac{a^{\alpha\beta} \mathbf{q}^{\alpha\beta}}{\left(\theta^{\alpha\beta}\right)^2} - \frac{1}{\theta^s} \sum_{\alpha\beta} \frac{\hat{Q}^{\alpha\beta}_{\alpha\beta\gamma} \theta^{\alpha\beta, s}}{\theta^{\alpha\beta}} \\
&- \frac{1}{\theta^s} \sum_{\alpha\beta} \hat{e}^{\alpha\beta}_{\alpha\beta\gamma} \left[\left(A^{\alpha\beta, s} - \frac{\gamma^{\alpha\beta}}{\Gamma^{\alpha\beta}} - \frac{p^s}{\rho^s} \right) + \frac{1}{2} (\mathbf{w}^{\alpha\beta, s})^2 + \eta^{\alpha\beta} \theta^{\alpha\beta, s} + \frac{\theta^{\alpha\beta, s}}{\theta^{\alpha\beta}} \frac{\gamma^{\alpha\beta}}{\Gamma^{\alpha\beta}} \right] \\
&+ \sum_{\alpha} \sum_{\alpha\beta} \frac{1}{\theta^{\alpha\beta}} \left\{ \hat{e}^{\alpha}_{\alpha\beta} \left[G^{\alpha\beta, \alpha} + \frac{1}{2} (\mathbf{w}^{\alpha\beta, \alpha})^2 \right] \right\} + \sum_{\alpha} \sum_{\alpha\beta} \left\{ \hat{Q}^{\alpha}_{\alpha\beta} \frac{\theta^{\alpha\beta, s}}{\theta^{\alpha\beta} \theta^{\alpha}} \right\} \\
&- \sum_{\alpha} \sum_{\alpha\beta} \left\{ \hat{Q}^{\alpha}_{\alpha\beta} \frac{\theta^{\alpha, s}}{\theta^{\alpha\beta} \theta^{\alpha}} \right\} + \sum_{\alpha} \sum_{\alpha \neq \beta} \left[\frac{\hat{e}^{\alpha}_{\alpha\beta}}{\theta^{\alpha\beta} \theta^{\alpha}} \left(\eta^{\alpha} \theta^{\alpha} - \frac{p^{\alpha}}{\rho^{\alpha}} \right) \theta^{\alpha\beta, \alpha} \right] \geq 0 \quad \text{(A-3)}
\end{aligned}
$$

As further simplification, we assume that there is no mass exchange between phases and consider local thermal equilibrium (so that $\theta^{\alpha} = \theta^{\alpha\beta} = \theta$):

$$
\begin{aligned}
\sum (\Lambda^{\alpha} + \Lambda^{\alpha\beta}) \theta = &- \sum_{\alpha} \varepsilon^{\alpha} \rho^{\alpha} \frac{\mathrm{D}^{\alpha} \theta}{\mathrm{D}t} \left\{ \eta^{\alpha} + \frac{\partial A^{\alpha}}{\partial \theta} \right\} - \sum_{\alpha\beta} a^{\alpha\beta} \Gamma^{\alpha\beta} \frac{\mathrm{D}^{\alpha\beta} \theta}{\mathrm{D}t} \left\{ \eta^{\alpha\beta} + \frac{\partial A^{\alpha\beta}}{\partial \theta} \right\} \\
&+ \sum_{\alpha \neq s} \mathbf{d}^{\alpha} : \left\{ \varepsilon s^{\alpha} \left(p^{\alpha} \mathbf{I} + \mathbf{t}^{\alpha} \right) \right\} \\
&+ (1-\varepsilon) \mathbf{d}^{s} : \Bigg\{ -\rho^{s} (Grad\ \mathbf{F}^{s})^{T} \cdot \frac{\partial A^{s}}{\partial \mathbf{E}^{s}} \cdot (Grad\ \mathbf{F}^{s}) + p^{s} \mathbf{I} + \mathbf{t}^{s} \\
&- a^{wn} \Gamma^{wn} \left(\frac{\partial A^{wn}}{\partial \varepsilon} \right) \mathbf{I} \Bigg\} + \dot{\varepsilon} \left[s^{n} p^{n} + s^{w} p^{w} - p^{s} \right] \\
&+ \sum_{\alpha} \mathbf{v}^{\alpha, s} \cdot \left[p^{\alpha} \nabla (\varepsilon s^{\alpha}) - \varepsilon s^{\alpha} \rho^{\alpha} \frac{\partial A^{\alpha}}{\partial s^{\alpha}} \nabla (s^{\alpha}) - \sum_{\alpha \neq \beta} \hat{\mathbf{T}}^{\alpha}_{\alpha\beta} \right] \\
&+ \sum_{\alpha\beta} \mathbf{w}^{\alpha\beta, s} \cdot \Bigg[-a^{\alpha\beta} \Gamma^{\alpha\beta} \left(\frac{\partial A^{\alpha\beta}}{\partial s^{w}} \right) \nabla (s^{w}) \\
&- \nabla (a^{\alpha\beta}) \left(\gamma^{\alpha\beta} + a^{\alpha\beta} \Gamma^{\alpha\beta} \frac{\partial A^{\alpha\beta}}{\partial a^{\alpha\beta}} \right) + \hat{\mathbf{T}}^{\alpha}_{\alpha\beta} + \hat{\mathbf{T}}^{\beta}_{\alpha\beta} - \hat{\mathbf{S}}^{\alpha\beta}_{\alpha\beta\gamma} \Bigg] \\
&+ \mathbf{w}^{wn, s} \left[-\nabla (\varepsilon) \left(a^{wn} \Gamma^{wn} \left(\frac{\partial A^{wn}}{\partial \varepsilon} \right) \right) \right] + \dot{s}^{w} \Bigg[\varepsilon p^{w} - \varepsilon p^{n} - \varepsilon s^{w} \rho^{w} \frac{\partial A^{w}}{\partial s^{w}} \\
&+ \varepsilon s^{n} \rho^{n} \frac{\partial A^{n}}{\partial s^{n}} - (1-\varepsilon) \rho^{s} \frac{\partial A^{s}}{\partial s^{w}} - \sum_{\alpha\beta} \Gamma^{\alpha\beta} a^{\alpha\beta} \left(\frac{\partial A^{\alpha\beta}}{\partial s^{w}} \right) \Bigg] \\
&+ \sum_{\alpha\beta} \mathbf{d}^{\alpha\beta} : \left\{ a^{\alpha\beta} (\mathbf{s}^{\alpha\beta} - \gamma^{\alpha\beta} \mathbf{I}) \right\} - \dot{a}^{wn} \left[a^{wn} \Gamma^{wn} \frac{\partial A^{wn}}{\partial a^{wn}} + \gamma^{wn} \right]
\end{aligned}
$$

$$- \sum_{\alpha\beta=ws,ns} \dot{a}^{\alpha\beta} \left[a^{\alpha\beta}\Gamma^{\alpha\beta} \frac{\partial A^{\alpha\beta}}{\partial a^{\alpha\beta}} + \gamma^{\alpha\beta} + (1-\varepsilon)\rho^s \frac{\partial A^s}{\partial a^{\alpha\beta}} \right]$$
$$+ \frac{\nabla\theta}{\theta} \cdot \left(\sum_{\alpha} \varepsilon^{\alpha} \mathbf{q}^{\alpha} + \sum_{\alpha\beta} a^{\alpha\beta} \mathbf{q}^{\alpha\beta} \right) \geq 0 \tag{A-4}$$

In r.h.s of Eq. (A-4) variables such as $\mathrm{D}^{\alpha\beta}\theta/\mathrm{D}t$, $\mathrm{D}^{\alpha}\theta/\mathrm{D}t$, $\mathbf{d}^{\alpha}$, and $\mathbf{d}^{\alpha\beta}$ appear linearly. This is because none of the constitutive functions were assumed to depend on these variables. For the entropy inequality to be valid for all thermodynamics states, coefficients of these variables should be identically zero. This gives, among other results, the following relationship for the solid stress tensor as:

$$\mathbf{t}^s = \rho^s (\mathrm{Grad}\ \mathbf{F}^s)^T \cdot \frac{\partial A^s}{\partial \mathbf{E}^s} \cdot (\mathrm{Grad}\ \mathbf{F}^s) - p^s \mathbf{I} + a^{wn}\Gamma^{wn} \left(\frac{\partial A^{wn}}{\partial \varepsilon} \right) \mathbf{I} \tag{A-5}$$

As well as an equilibrium equation for solid pressure, p^s :

$$p^s = s^n p^n + s^w p^w \tag{A-6}$$

The equations for solid stress tensor and solid pressure (A-5 and A-6) can be combined and rewritten to provide the following form for the effective stress tensor:

$$\mathbf{t}^e = (\mathbf{t}^s - P^n \mathbf{I}) + s^w P_c \mathbf{I} - a^{wn}\Gamma^{wn} \left(\frac{\partial A^{wn}}{\partial \varepsilon} \right) \mathbf{I} \tag{A-7}$$

Appendix B: Exploitation of Entropy Inequality for Deformable Solid:

$$\begin{aligned} A^s &= A^s(\rho^s, \mathbf{E}^s, \theta^s, s^w) \\ A^{\alpha} &= A^{\alpha}(\rho^{\alpha}, \theta^{\alpha}, s^{\alpha}) \\ A^{ws} &= A^{ws}(\Gamma^{ws}, \theta^{ws}, s^w, a^{ws},\ \varepsilon) \\ A^{ns} &= A^{ns}(\Gamma^{ns}, \theta^{ns}, s^w, a^{ns},\ \varepsilon) \\ A^{wn} &= A^{wn}(\Gamma^{wn}, \theta^{wn}, s^w, a^{wn}, \varepsilon) \end{aligned} \tag{B-1}$$

Following the same procedure and mathematical manipulations presented in "Appendix A", the following form for entropy inequality can be obtained (where no mass exchange between phases and interfaces exist and local thermal equilibrium holds):

$$\begin{aligned} \sum (\Lambda^{\alpha} + \Lambda^{\alpha\beta})\theta = &- \sum_{\alpha} \varepsilon^{\alpha}\rho^{\alpha} \frac{\mathrm{D}^{\alpha}\theta}{\mathrm{D}t} \left\{ \eta^{\alpha} + \frac{\partial A^{\alpha}}{\partial \theta} \right\} - \sum_{\alpha\beta} a^{\alpha\beta}\Gamma^{\alpha\beta} \frac{\mathrm{D}^{\alpha\beta}\theta}{\mathrm{D}t} \left\{ \eta^{\alpha\beta} + \frac{\partial A^{\alpha\beta}}{\partial \theta} \right\} \\ &+ \sum_{\alpha \neq s} \mathbf{d}^{\alpha} : \{ \varepsilon s^{\alpha} \left(p^{\alpha}\mathbf{I} + \mathbf{t}^{\alpha} \right) \} \\ &+ (1-\varepsilon)\ \mathbf{d}^s : \left\{ -\rho^s (Grad\ \mathbf{F}^s)^T \cdot \frac{\partial A^s}{\partial \mathbf{E}^s} \cdot (Grad\ \mathbf{F}^s) + p^s \mathbf{I} + \mathbf{t}^s \right. \\ &\left. - \sum_{\alpha\beta} \frac{a^{\alpha\beta}\Gamma^{\alpha\beta s}}{\alpha\beta} \left(\frac{\partial A^{\alpha\beta}}{\partial \varepsilon} \right) \mathbf{I} \right\} + \dot{\varepsilon} \left[s^n p^n + s^w p^w - p^s \right] \end{aligned}$$

$$
\begin{aligned}
&+\sum_{\alpha}\mathbf{v}^{\alpha,s}\cdot\left[p^{\alpha}\nabla(\varepsilon s^{\alpha})-\varepsilon s^{\alpha}\rho^{\alpha}\frac{\partial A^{\alpha}}{\partial s^{\alpha}}\nabla(s^{\alpha})-\sum_{\alpha\neq\beta}\hat{\mathbf{T}}^{\alpha}_{\alpha\beta}\right]\\
&+\sum_{\alpha\beta}\mathbf{w}^{\alpha\beta,s}\cdot\left[-a^{\alpha\beta}\Gamma^{\alpha\beta}\left(\frac{\partial A^{\alpha\beta}}{\partial s^{w}}\right)\nabla(s^{w})\right.\\
&-\nabla(a^{\alpha\beta})\left(\gamma^{\alpha\beta}+a^{\alpha\beta}\Gamma^{\alpha\beta}\frac{\partial A^{\alpha\beta}}{\partial a^{\alpha\beta}}\right)+\hat{\mathbf{T}}^{\alpha}_{\alpha\beta}+\hat{\mathbf{T}}^{\beta}_{\alpha\beta}\\
&\left.-\hat{\mathbf{S}}^{\alpha\beta}_{\alpha\beta\gamma}-a^{\alpha\beta}\Gamma^{\alpha\beta}\left(\frac{\partial A^{\alpha\beta}}{\partial\varepsilon}\right)\nabla(\varepsilon)\right]-\sum_{\alpha\beta}a^{\alpha\beta}\Gamma^{\alpha\beta}\left(\frac{\partial A^{\alpha\beta}}{\partial\varepsilon}\right)\dot{\rho}^{s}\\
&+\dot{s}^{w}\left[\varepsilon p^{w}-\varepsilon p^{n}-\varepsilon s^{w}\rho^{w}\frac{\partial A^{w}}{\partial s^{w}}+\varepsilon s^{n}\rho^{n}\frac{\partial A^{n}}{\partial s^{n}}-(1-\varepsilon)\rho^{s}\frac{\partial A^{s}}{\partial s^{w}}\right.\\
&\left.-\sum_{\alpha\beta}\Gamma^{\alpha\beta}a^{\alpha\beta}\left(\frac{\partial A^{\alpha\beta}}{\partial s^{w}}\right)\right]+\sum_{\alpha\beta}\mathbf{d}^{\alpha\beta}:\left\{a^{\alpha\beta}(\mathbf{s}^{\alpha\beta}-\gamma^{\alpha\beta}\mathbf{I})\right\}\\
&-\dot{a}^{wn}\left[a^{wn}\Gamma^{wn}\frac{\partial A^{wn}}{\partial a^{wn}}+\gamma^{wn}\right]\\
&-\sum_{\alpha\beta=ws,ns}\dot{a}^{\alpha\beta}\left[a^{\alpha\beta}\Gamma^{\alpha\beta}\frac{\partial A^{\alpha\beta}}{\partial a^{\alpha\beta}}+\gamma^{\alpha\beta}+(1-\varepsilon)\rho^{s}\frac{\partial A^{s}}{\partial a^{\alpha\beta}}\right]\\
&+\frac{\nabla\theta}{\theta}\cdot\left(\sum_{\alpha}\varepsilon^{\alpha}\mathbf{q}^{\alpha}+\sum_{\alpha\beta}a^{\alpha\beta}\mathbf{q}^{\alpha\beta}\right)\geq 0
\end{aligned}
\tag{B-2}
$$

After further simplification, application of the constitutive assumptions is the last step which asserts terms inside braces in the most simplified form should be zero. This leads to the following form for the effective stress tensor in a granular porous medium with deformable grains:

$$
\mathbf{t}^{e}=(\mathbf{t}^{s}-P^{n}\mathbf{I})+s^{w}(P_{c}\mathbf{I})-\sum_{\alpha\beta}\left(\frac{\partial A^{\alpha\beta}}{\partial\varepsilon}\Gamma^{\alpha\beta}a^{\alpha\beta}\right)\mathbf{I}
\tag{B-3}
$$

Appendix C: On the Relationship Connecting Effective Stress Parameter to the Area Between Soil Water Retention Curve and Saturation Axis

Grant and Gerhard (2007) suggested the following relationship to determine the wetting–nonwetting interfacial area:

$$
a^{wn}=\psi(s^{w}).\,E_{d}.\,\frac{\varepsilon}{\sigma^{nw}}\int_{s^{w}=s^{wi}}^{s^{w}=1}P_{c}ds^{w,d}\qquad\text{For drying branch}
\tag{C-1}
$$

$$
a^{wn}=\psi(s^{w}).\,E_{d}.\,\frac{\varepsilon}{\sigma^{nw}}\left[\int_{s^{w}=s^{wx}}^{s^{w}=1}P_{c}ds^{w,d}-\int_{s^{w}=s^{wx}}^{s^{w}=s^{wi}}P_{c}ds^{w,im}\right]\text{For wetting (main/scannings)}
\tag{C-2}
$$

where s^{wi} denotes saturation at a point on drying or wetting at which the value of wetting-nonwetting specific interfacial area is sought. s^{wx} is the degree of saturation at which suction reversal occurs and wetting starts. E_d is a coefficient which accounts for energy dissipation occurring due to the roughness of grain surface. E_d is equal to unity in an ideal case where the whole mechanical work given to the soil system is transformed to the interfacial energy. ψ is a function which shows the portion of nonwetting interface which is in contact with wetting phase. In integrands, *im* denotes integrating on imbibition curves (wetting) and d specifies integration along drying path of SWRC. σ^{nw} is the interfacial tension between wetting and non-wetting phases (air and water in unsaturated soil system).

The integration appearing in the Eqs. (C-1) and (C-2) gives the total air interface created in the soil system. It includes air-solid interface as well as air–water interface. Because we are interested to know the amount of air–water interfaces, this ψ function appears. Grant and Gerhard (2007) considered ψ to be a function of saturation only. However, they pointed out that it can also depend on the capillary pressure, in general.

These two equations show that the amount of specific air–water interfacial area is related to the area between soil water retention curve and saturation axis for drying branch. During wetting, the amount of non-wetting interfaces decrease proportional to the area under the wetting path (from suction reversal point to the current state of saturation). Substitution of (C-1) and (C-2) into Eq. 22 gives the following relationship for the effective stress parameter:

$$\chi = s^w + \frac{K(s^w, P_c, \varepsilon) \int_{s^w=s^{wi}}^{s^w=1} P_c ds^{w,d}}{P_c} \quad \text{For drying branch} \tag{C-3}$$

$$\chi = s^w + \frac{K(s^w, P_c, \varepsilon) \left[\int_{s^w=s^{wx}}^{s^w=1} P_c ds^{w,d} - \int_{s^w=s^{wx}}^{s^w=s^{wi}} P_c ds^{w,im} \right]}{P_c} \quad \text{For wetting branch} \tag{C-4}$$

where $K(s^w, P_c, \varepsilon) = k^{wn}.\psi.\ E_d.\ \frac{\varepsilon}{\sigma^{nw}}$

References

Alonso, E.E., Pereira, J.M., Vaunat, J., Olivella, S.: A microstructurally based effective stress for unsaturated soils. Geotechnique **60**, 913–925 (2010)

Bishop, A.W.: The principle of effective stress. Teknisk Ukeblad **39**, 859–863 (1959)

Bishop, A.W., Blight, G.E.: Some aspects of effective stress in saturated and partly saturated soils. Geotechnique **13**(3), 177–197 (1963)

Blight, G.E.: Strength and consolidation characteristics of compacted soils. PhD Dissertation, University of London (1961)

Borja, R.I.: On the mechanical energy and effective stress in saturated and unsaturated porous continua. Int. J. Solids Struct. **43**, 1764–1786 (2006)

Bowen, R.M.: Porous media model formulations by the theory of mixtures. In: Bear, J., corapcioglu, M.Y. (eds.) Fundamentals of Transport Phenomena in Porous Media, pp. 199–256. Martinus Nijhoff Publishers, Dordrecht (1984)

Cammarata, R.C., Sieradzki, K.: Surface and interface stresses. Annu. Rev. Mater. Sci. **24**, 215–234 (1994)

Chateau, X., Dormieux, L.: Micromechanics of saturated and unsaturated porous media. Int. J. Numer. Anal. Methods Geomech. **26**, 831–844 (2002)

Chhapadia, P., Mohammadi, P., Sharma, P.: Curvature-dependent surface energy and implications for nanostructures. JMPS **59**(10), 2103–2115 (2011)

Coussy, O.: Revisiting the constitutive equations of unsaturated porous solids using a Lagrangian saturation concept. Int. J. Numer. Anal. Methods Geomech. **31**, 1675–1694 (2007)

Coussy, O.: Mechanics and Physics of Porous Solids. Wiley, Chichester (2010)

Coussy, O., Dangla, P.: Approche énergétique du comportement des sols non saturés. In: Coussy, O., Fleureau, J.-M. (eds.) Mécanique des sols non saturés., pp. 137–174. Hermès, Paris (2002)
Culligan, K.A., Wildenschild, D., Christensen, B.S.B., Gray, W.G., Rivers, M.L.: Pore-scale characteristics of multiphase flow in porous media: a synchrotron-based cmt comparison of air–water and oil-water experiments. Adv. Water Res. **29**(2), 227–238 (2006)
Eriksson, J.C., Ljunggren, S.: Is it necessary that the interfacial tension of a general curved interface is constant along the interface at equilibrium?. J. Colloid Interface Sci. **152**(2), 575–577 (1992)
Eringen, A.C.: Mechanics of Continua. Krieger, New York (1980)
Fredlund, D.G., Xing, A.: Equations for the soil–water characteristic curve. Can. Geotech. J. **31**, 521–532 (1994)
Grant, G.P., Gerhard, J.I.: Simulating dissolution of a complex dense non-aqueous phase liquid source zone: 1. Model to predict interfacial area. Water Resour. Res. **43**(W12410):1–14 (2007)
Gray, W.G., Hassanizadeh, S.M.: Averaging theorems and averaged quantities for transport of interface properties in multiphase systems. Int. J. Multiphase Flow **15**, 81–95 (1989)
Gray, W.G., Schrefler, B.A.: Thermodynamic approach to effective stress in partially saturated porous media. Eur. J. Mech. A/Solids **20**, 521–538 (2001)
Gray, W.G., Schrefler, B.A., Pesavento, F.: The solid stress tensor in porous media mechanics and the Hill-Mandel condition. JMPS **57**, 539–544 (2009)
Gurtin, M.E., Jabbour, M.E: Interface evolution in three-dimensions with curvature-dependent energy and surface diffusion: interface-controlled evolution, phase transitions, epitaxial growth of elastic films. Arch. Ration. Mech. Anal. **163**, 171–208 (2002)
Gurtin, M.E., Murdoch, A.I.: A continuum theory of elastic material surfaces. Arch. Ration. Mech. Anal. **57**, 291–323 (1974)
Hassanizadeh, S.M.: Continuum description of thermodynamic processes in porous media: Fundamentals and applications. In: Kublik, J., Kaczmarek, M., Murdoch, I. (eds.) Modeling Coupled Phenomena in Saturated Porous Materials, pp. 179–223. Institute of Fundamental Technological Research, Polish Academy of Sciences, Warsaw (2003)
Hassanizadeh, S.M., Gray, W.G.: General conservation equations for multi-phase systems: 2. Mass, momentum, energy, and entropy equations. Adv. Water. Res. **2**, 191–203 (1979)
Hassanizadeh, S.M., Gray, W.G.: Mechanics and thermodynamics of multiphase flow in porous media including interphase boundaries. Adv. Water. Res. **13**, 169–186 (1990)
Hassanizadeh, S.M., Gray, W.G.: Thermodynamic basis of capillary pressure in porous media. Water Resour. Res. **29**, 3389–3405 (1993)
Houlsby, G.T.: Work input to an unsaturated granular material. Geotechnique **47**, 193–196 (1997)
Hutter, K., Laloui, L., Vulliet, L.: Thermodynamically based mixture models of saturated and unsaturated soils. Mech. Cohesive-Frict. Mater. **4**, 295–338 (1999)
Joekar-Niasar, V., Hassanizadeh, S.M., Leijnse, A.: Insights into the relationships among capillary pressure, saturation, interfacial area and relative permeability using pore-network modeling. Transp. Porous Med. **74**, 201–219 (2008)
Jommi, C., di Prisco, C.: Un semplice approccio teorico per la modellazione del comportamento meccanico dei terreni granulari parzialmente saturi. Atti Convegno sul Tema: Il Ruolo dei Fluidi nei Problemi di Ingegneria Geotecnica, Mondovì, 167–188 (1994)
Khalili, N., Geiser, F., Blight, G.E.: Effective stress in unsaturated soils, a review with new evidence. Int. J. Geomech. **4**(2), 115–126 (2004)
Khalili, N., Habte, M.A., Zargarbashi, S.: A fully coupled flow deformation model for cyclic analysis of unsaturated soils including hydraulic and mechanical hystereses. Comput. Geotech. **35**, 872–889 (2008)
Khalili, N., Khabbaz, M.H.: A unique relationship for χ for the determination of the shear strength of unsaturated soils. Géotechnique **48**, 1–7 (1998)
Khalili, N., Zargarbashi, S.: Influence of hydraulic hysteresis on effective stress in unsaturated soils. Géotechnique **60**(9), 729–734 (2010)
Kohgo, Y., Nakano, M., Miyazaki, T.: Theoretical aspects of constitutive modeling for unsaturated soils. Soils Found. **33**(4), 49–63 (1993)
Laloui, L., Nuth, M.: On the use of the generalised effective stress in the constitutive modelling of unsaturated soils. Comput. Geotech. **36**, 20–23 (2008)
Loret, B., Khalili, N.: A three-phase model for unsaturated soils. Int. J. Numer. Anal. Methods Geomech. **24**, 893–927 (2000)
Lu, N., Godt, J.W., Wu, D.T.: A closed form equation for effective stress in unsaturated soils. Water Resour. Res. **46**(5) (2010). doi:10.1029/2009WR008646
Lu, N., Likos, W.J.: Suction stress characteristic curve for unsaturated soil. ASCE J. Geotech. Geoenviron. Eng. **132**(2), 131–142 (2006)

Masın, D.: Predicting the dependency of a degree of saturation on void ratio and suction using effective stress principle for unsaturated soils. Int. J. Numer. Anal. Methods Geomech. **34**, 73–90 (2010)
Matyas, E.L., Radhakrishna, H.S.: Volume change characteristics of partially saturated soils. Géotechnique **18**(4), 432–448 (1968)
Murdoch, A.I., Hassanizadeh, S.M.: Macroscale balance relations for bulk, interfacial and common line systems in multiphase flows through porous media on the basis of molecular considerations. Int. J. Multiph. Flow **28**, 1091–1123 (2002)
Nikooee, E.: A thermodynamics approach to effective stress parameter in unsaturated soils considering net stress effects. PhD Dissertation, Department of Civil and Environmental Engineering, Shiraz University (2012)
Nikooee, E., Habibagahi, G., Hassanizadeh, S.M., Ghahramani, A.: Effective stress in unsaturated soils: insights from thermodynamics. In: 2nd European Conference on Unsaturated Soils, Naples, Italy, (2012)
Nuth, M., Laloui, L.: Effective stress concept in unsaturated soils: clarification and validation of a unified framework. Int. J. Numer. Anal. Methods Geomech. **32**, 771–801 (2008)
Nuth, M., Laloui, L.: Advances in modeling hysteretic water retention curve in deformable soils. Comput. Geotech. **35**(6), 835–844 (2008)
Pereira, J.M., Coussy, O., Alonso, E.E., Vaunat, J., Olivella, S.: Is the degree of saturation a good candidate for Bishop's parameter?. In: Alonso, E.E., Gens, A. (eds.) Unsaturated Soils—Proceedings of 5th International Conference on Unsaturated Soils, vol. 2, pp. 913–919. CRC Press, Barcelona (2010)
Schrefler, B.A.: The finite element method in soil consolidation (with application to surface subsidence). Ph.D. Dissertation, University College of Swansea (1984)
Scriven, L.E.: Dynamics of a fluid interface: equation of motion for Newtonian surface fluids. Chem. Eng. Sci. **12**, 92–108 (1960)
Spaepen, F.: Interfaces and stresses in thin film. Acta Mater. **48**, 31–42 (2000)
Terzaghi, K: The shear resistance of saturated soils. In: Casagrande, A., Rutledge, P.C., Watson, J.D. (eds.) Proceedings of 1st International Conference on Soil Mechanics and Foundation Engineering, Cambridge, Massachusetts, pp. 54–56. Harvard University Press, USA (1936)
Terzaghi, K.: Theoretical Soil Mechanics. Wiley, New York (1943)
Uchaipichat, A.: Prediction of shear strength for unsaturated soils under drying and wetting processes. Electron. J. Geotech. Eng. (EJGE) **15**(K), 1087–1102 (2010)
Uchaipichat, A.: Influence of hydraulic hysteresis on effective stress in unsaturated clay. Int. J. Environ. Earth. Sci. **1**, 20–24 (2010)
Uchaipichat, A.: A hydro-mechanical model for unsaturated soils. Proc. World Acad. Sci. Eng. Tech. **68**, 202–206 (2010)
Zhao, C.G., Liu, Y., Gao, F.P.: Work and energy equations and the principle of generalised effective stress for unsaturated soils. Int. J. Numer. Anal. Methods Geomech. **34**, 920–936 (2010). doi:10.1002/nag.839